REVIEW

Check for updates

DNA attachment to polymeric, soft and quantum materials: mechanisms and applications

Mohamad Zandieh, [a] Jung Heon Lee [b] and Juewen Liu [*a]

Polymeric and soft materials offer excellent biocompatibility, a high capacity for loading of guest molecules, and cost-effectiveness. Additionally, recent studies on nanodiamonds as quantum materials have revealed interesting applications at ambient temperatures. The attachment of DNA oligonucleotides to these materials enables molecular recognition, directed assembly and targeting capabilities, offering unique advantages for biomedical, analytical and environmental applications. In this article, the mechanisms of DNA adsorption to various metal-free materials, including polydopamine (PDA), hydrogels, microplastics, cellulose crystals, nanodiamonds, and carbon quantum dots are reviewed. Key interactions involved in these systems include $\pi-\pi$ stacking, hydrogen bonding, hydrophobic interactions, and metal bridging. We highlight how material properties such as surface charge, functional groups, and wettability influence DNA adsorption and release. Stimuli-responsive systems, such as pH-switchable PDA and thermoresponsive hydrogels, allow controlled DNA adsorption and release. Furthermore, sequence-specific aptamers developed for microplastics and cellulose are discussed, demonstrating the potential for selective DNA binding to nanomaterials. Finally, applications including fluorescence-based biosensors, intracellular delivery, high-density DNA storage, and surface probing are presented. Remaining challenges and future directions are also discussed to guide further advancements in this emerging field.

1. Introduction

The attachment of DNA oligonucleotides to inorganic nanomaterials,[1–3] such as gold, quantum dots, and metal oxides, have enabled the development of various biosensors, drug delivery vehicles, and stimuli-responsive materials.[4–7] DNA provides molecular recognition capabilities, while nanomaterials enable signal transduction, drug loading, and DNA protection. Beyond recognizing complementary nucleic acids, DNA can also recognize metal ions, small molecules, proteins, cells, and surfaces through the aptamer technology.[8–12] Aptamers are single-stranded DNA or RNA oligonucleotides that selectively bind to target molecules. DNA aptamers are preferred for materials-related applications due to their significantly greater stability than RNA (approximately one million times higher).[13] Additionally, DNA is more cost-effective to produce and easier for covalent modifications for bioconjugation and signal transduction.

DNA can adsorb to metal-containing nanomaterials through various interactions. For instance, DNA nucleobases strongly coordinate with gold nanoparticles (AuNPs),[14] the phosphate backbone binds effectively to different metal oxide NPs,[15] and van der Waals forces facilitate the adsorption of DNA to WS_2 and MoS_2.[16–19] However, metal-containing nanomaterials pose potential toxicity concerns due to the metal species. Many other important materials do not contain metal ions. For *in vivo* applications, metal-free materials are more attractive and more likely to be approved for clinical use. Currently, most FDA-approved nanomaterials for drug delivery are based on liposomes and biodegradable polymers, with only a few incorporating biocompatible metals such as calcium and iron.[20]

Polydopamine (PDA) is widely used for coating various surfaces due to its excellent adhesive properties.[21,22] Hydrogels, composed of crosslinked hydrophilic polymer networks capable of retaining a large fraction of water, are valuable for designing smart soft materials especially for biomedical applications due to their excellent biocompatibility and stimuli-responsiveness.[23,24] Some polymeric materials, however, raise environmental and health concerns. Recently, microplastics received significant attention due to their accumulation in animals and humans, which can lead to diseases.[25–27] Another class of intriguing materials is quantum materials, such as fluorescent nanodiamond containing nitrogen vacancies, which are of particular interest for sensing and imaging applications.[28] Understanding and controlling DNA adsorption to these materials can offer new functionalities. These materials, being free of metal species, interact with DNA *via* alternative forces such as

a Department of Chemistry, Waterloo Institute for Nanotechnology, University of Waterloo, Waterloo, ON, N2L 3G1, Canada. E-mail: liujw@uwaterloo.ca

b School of Advanced Materials Science and Engineering, Sungkyunkwan University (SKKU), Suwon 16419, Republic of Korea

π–π stacking, hydrophobic interactions, and van der Waals interactions. While metal coordination may still occur, it typically involves externally added metal ions acting as bridges.[29]

DNA oligonucleotides can interact with materials *via* either covalent conjugation or physical adsorption. In terms of adsorption, two distinct types exist. One is nonspecific adsorption, where DNA sequence does not play a major role, and sequences with similar base compositions generally exhibit a comparable adsorption strength. Due to polyvalent interactions along a DNA chain, such nonspecific adsorption can be quite strong. The other type is specific sequence-dependent adsorption. In this case, strongly adsorbing sequences can be regarded as aptamers for the surface or material,[30] and mutations in aptamer sequence may decrease the adsorption affinity. For certain applications, such as targeted drug delivery and biosensors, it is important to form a stable bioconjugate while minimizing DNA/material interactions to retain the targeting ability of DNA aptamers.[31,32] In contrast, for applications such as DNA extraction, strong DNA/material interactions are desirable, even in complex sample matrices. Therefore, it is critical to precisely control the interaction strength, which requires a comprehensive understanding of the underlying interaction mechanisms.

While numerous review papers have discussed DNA conjugation to various inorganic nanomaterials from AuNPs,[33–35] metal oxide NPs[36,37] to MXenes,[38] no comprehensive reviews have yet covered polymeric and soft materials, especially with a focus on fundamental interaction mechanisms. To address this gap, we selected a diverse set of polymeric and soft materials, including PDA, hydrogels, microplastics, nanodiamonds (NDs), cellulose nanocrystals (CNC), and carbon quantum dots (CQDs), based on their growing relevance in biomedical, environmental, and nanotechnology applications, as well as their distinct physicochemical properties that influence DNA interactions. Since graphene oxide has already been extensively reviewed for DNA adsorption due to its high surface area and versatile functionalization capabilities,[39,40] we did not include it here. While this review covers a relatively long timeframe, particular emphasis is placed on studies published within the past decade.

2. Competing interactions for DNA adsorption

Fig. 1a shows the structure of the four nucleobases, and a scheme of a single-stranded DNA (ssDNA), which is highly flexible due to the presence of many rotatable bonds in a phosphodiester backbone. The persistence length of a ssDNA is approximately only 0.7 nm.[41] In contrast, the persistence length of a double-stranded DNA is approximately 50 nm. Therefore, ssDNA can more easily form conformal adsorption structures. Among the four nucleobases, adenine and guanine are purines, and they can have stronger π–π stacking interactions.[42] Guanine, being the most hydrophobic base among the
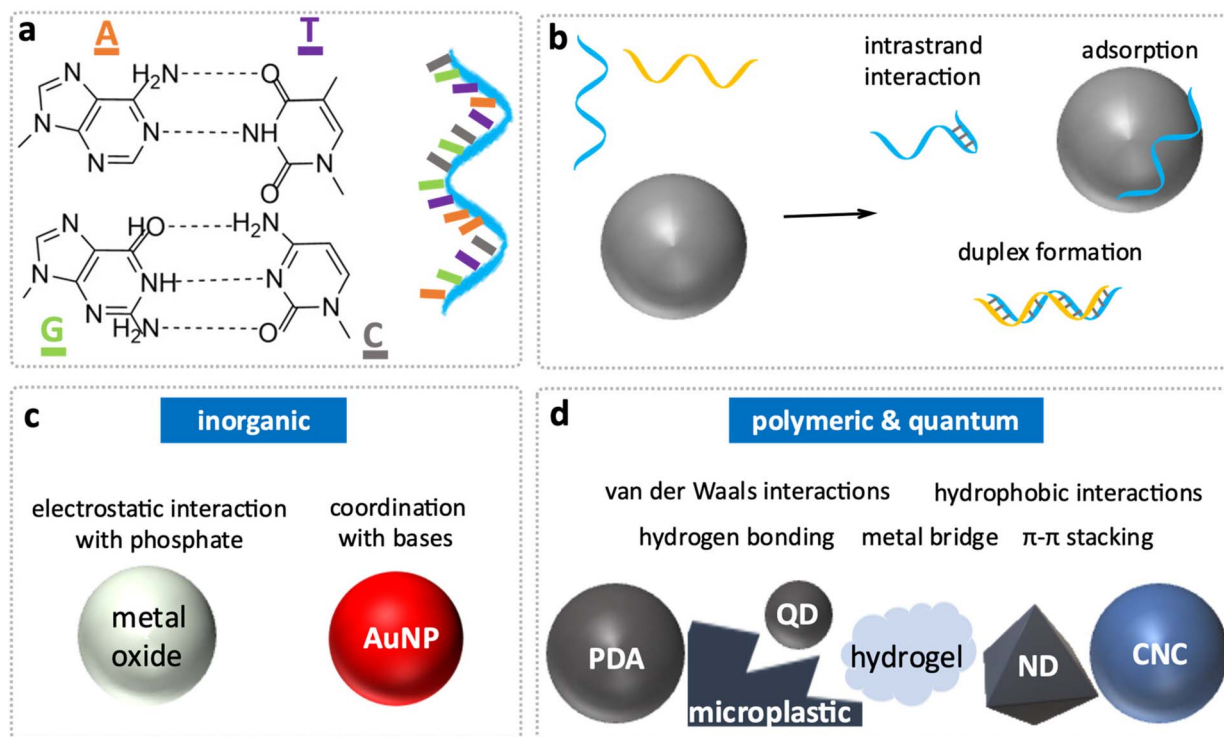

Fig. 1 (a) A scheme depicting a ssDNA consisting of a phosphate backbone and nucleobases, along with the structures of the four nucleobases: adenine (A), thymine (T), guanine (G), and cytosine (C). (b) Competition between DNA intrastrand interactions, duplex formation, and adsorption. (c) Interaction forces involved in DNA adsorption to metal-containing nanomaterials, such as metal oxides and AuNPs. (d) Interaction forces involved in DNA adsorption on various polymeric and quantum materials.

four, may play an important role when a DNA interacts with hydrophobic surfaces.[43] However, DNA with a high purine content may also exhibit more intramolecular interactions, folding into various internal secondary structures, which in turn can reduce DNA/surface interactions.

An ssDNA oligonucleotide can engage in several types of interactions (Fig. 1b). First, it can interact with itself to form certain secondary structures. Depending on its sequence, the DNA may adapt a single stable structure or various meta-stable structures that may inter-convert. Second, it can interact with its complementary DNA to form a duplex, which hides the nucleobases and only exposes the phosphate backbone.[44] This single-to-double strand transition can drastically alter the interaction between DNA and nanomaterials. Third, DNA may interact with other molecules or surfaces, and surface interactions are the focus of this article. These three interactions compete with one another, and the final binding state is often determined by both thermodynamic and kinetic factors. For DNA capable of forming stable secondary structures, only a few nucleotides may be exposed. Although each exposed nucleotide may interact strongly with a surface, the overall adsorption may still be weak due to the limited number of available nucleotides. In contrast, a DNA that does not form stable secondary structures tends to have more exposed nucleotides, resulting in stronger overall adsorption.[45]

Fig. 1d shows some of the polymeric materials to be reviewed in this paper. While this list covers only a small subset of all available materials in this group, they are representative and have the most data regarding interactions with DNA. We aim to highlight different types of adsorption forces between these metal-free polymeric materials *versus* metal-containing inorganic NPs such as AuNPs and metal oxides (Fig. 1c).

3. Polydopamine

Polydopamine (PDA) is a synthetic mimic of melanin and can be spontaneously and robustly coated onto various substrates under mild conditions,[46,47] allowing for precise control over coating thickness and surface chemistry.[48] A generally accepted structure of PDA is shown in Fig. 2a, containing a high density of catechol and amine groups, facilitating versatile interactions with DNA *via* hydrogen bonding and π–π stacking. By
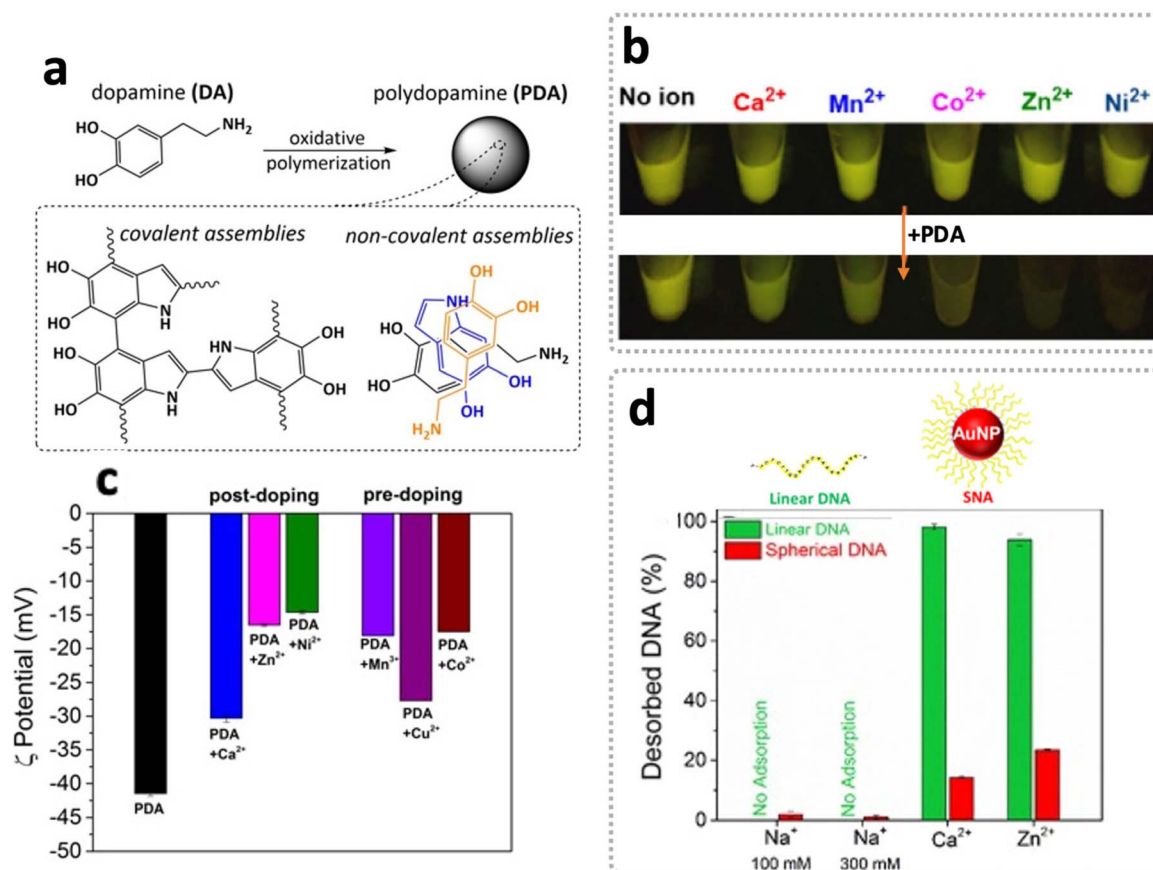

Fig. 2 (a) The structure of PDA, consisting of covalent and noncovalent assemblies of various oxidation products of dopamine. (b) Fluorescent micrographs depicting 100 nM FAM-labelled DNA mixed with 30 μM different metal ions in the absence or presence of 20 μg mL^{-1} PDA. Reproduced with permission.[53] Copyright 2020, American Chemical Society. (c) ζ-Potentials of PDA NPs showing a less negative surface charge when metal ions were added during or after the synthesis. Reproduced with permission.[55] Copyright 2020, Wiley-VCH. (d) Desorption of linear DNA and SNA from 50 μg mL^{-1} PDA (in the presence of 100 and 300 mM Na$^+$, 2 mM Ca^{2+}, or 0.6 mM Zn^{2+}) induced by 4 mM EDTA. Reproduced with permission.[56] Copyright 2020, American Chemical Society.

chemically modifying dopamine, the range of coatable surfaces can be further expanded. At physiological pH, PDA is negatively charged, and a direct attachment of DNA becomes difficult. To adsorb DNA, the charge repulsion between negatively charged DNA and PDA needs to be overcome.

3.1. Low pH-assisted DNA adsorption

PDA has an isoelectric point of 4.5, and thus lowering the pH can promote DNA adsorption. Below its isoelectric point, PDA becomes positively charged due to protonation, while DNA remains negatively charged above pH 2. This enables electrostatic attraction between DNA and PDA at low pH. The Jia group investigated the DNA adsorption efficiency on PDA over a wide pH range.[49,50] The maximum DNA adsorption capacity of 161 mg g^{-1} occurred at pH 2, and that 80% of the adsorbed DNA could be efficiently released at pH 8 due to the deprotonation of phenolic hydroxyl groups in PDA, which resulted in electrostatic repulsion between PDA surface and DNA.

3.2. Metal bridged adsorption

Another approach to promote DNA adsorption on PDA is through metal-mediated interactions, since both PDA[51] and DNA have multiple metal binding sites.[8] Divalent metal ions not only screen the charge repulsion between negatively charged DNA and PDA, but also mediate additional interactions, such as metal bridges, cation–π interactions and hydrogen bonding with hydrated metal ions.[52] Even though divalent metal ions have been commonly used in buffers for DNA adsorption on PDA, Meng et al. first systematically investigated the role of various metal ions. At pH 7.6, up to 200 mM of monovalent metal ions (Na$^+$ or K$^+$) did not induce DNA adsorption on PDA, whereas divalent metal ions (2 mM Mg^{2+} or Ca^{2+}) promoted adsorption, with Ca^{2+} being more effective than Mg^{2+}.

Later, our group investigated the effect of transition metal ions, and the DNA adsorption affinity followed the order of Ni^{2+} > Zn^{2+} > Co^{2+} > Mn^{2+} > Ca^{2+} (Fig. 2b).[53] The higher efficiency of transition metal ions may be attributed to their stronger affinity to DNA.[8] Our group also incorporated metal ions during the synthesis of PDA and achieved enhanced DNA adsorption efficiency and robustness.[54] Incorporating metal ions during the synthesis of PDA resulted in a less negative PDA surface charge, which can decrease repulsion to DNA (Fig. 2c).[55] Moreover, EDTA induced a complete desorption of preabsorbed DNA from PDA surface suggesting the critical role of metal ions for DNA adsorption on PDA at neutral pH. Polyphosphate and urea were other regents that induced DNA desorption from PDA surface,[53,56] implying the role of DNA phosphate backbone as well as hydrogen bonding for DNA adsorption on PDA.

3.3. Polyvalent binding

Alongside low pH and metal ions, another effective method for DNA adsorption on PDA is through polyvalent binding. The weak interactions between individual DNA oligonucleotides and PDA can be amplified when DNA is densely immobilized on an AuNP core (referred to as spherical DNA or SNA, Fig. 2d).[56] In this case, even a monovalent metal ion such as Na$^+$ could induce

DNA adsorption. The stability was higher than that of linear DNA adsorption, and at high metal concentrations, neither 4 M urea nor 4 mM EDTA could induce SNA desorption from PDA (Fig. 2d). Therefore, the stable adsorption implied that after the removal of metal ions, other forces maintained the adsorption. Hydrogen bonding and π–π interactions are examples of weak interactions that can be amplified by polyvalent binding, which is likely responsible for this extraordinarily stable adsorption.[57] Furthermore, the metal-dependent DNA adsorption curve suggested that cooperative binding of multiple metal ions was necessary for efficient adsorption.

PDA is a representative example of polymeric materials with aromatic surface groups and versatile functional moieties (e.g., catechols, amines) that enable diverse interactions with biomolecules like DNA. While other phenolic-rich polymers (e.g., tannic acid-based coatings[58]) share similar features, such as hydrogen bonding and metal affinity, PDA offers superior robustness in coating and tunable surface chemistry. These properties make PDA an ideal model system for studying the interplay of electrostatic, coordination, and π-driven interactions with DNA.

3.4. Covalent DNA attachment

DNA can also be covalently conjugated to PDA through thiol- or amine-modified DNA strands, leveraging the oxidation of dopamine's catechol groups to quinones, which undergo Michael addition with nucleophilic thiols or amines. The reaction efficiency depends on pH, with optimal conditions near or below the pK_a of the Michael acceptor (e.g., pH 8.5 for thiolated DNA and pH 7.5 for amine-modified DNA).[59,60] To maximize DNA loading density, a salt-aging step (adding NaCl up to 0.15 M) is employed to mitigate electrostatic repulsion between DNA strands,[59,60] a strategy adapted from AuNP functionalization.[2,61] While both Michael addition and Schiff-base reactions can occur, the former dominates due to the hydrolytic instability of imine bonds.[62,63] The resulting PDA–DNA conjugates exhibit exceptional stability, resisting DNA release even after 24 h at 75 °C across a broad pH range (2–11), with minimal detachment (~5%) observed only at pH 12.[59] This robustness is attributed to residual quinone moieties and electrophilic sites present in the PDA structure.[63]

4. Hydrogels

Hydrogels are three-dimensional, water-swollen polymer networks known for their biocompatibility and stimuli-responsiveness. They are also well suited for biomedical applications due to their tunable properties and a high biomolecule-loading capacity. Hydrogels can be made from a variety of polymers. Important hydrogel products include contact lens,[64] wound dressings,[65] sensors,[66–69] drug delivery systems,[70] tissue engineering scaffolds,[71] diapers,[72] hygiene products,[73] and soft robotics.[74] Numerous studies have reported covalent modification of hydrogels with DNA for applications in sensing, drug delivery and separation. Covalent attachment of DNA is typically achieved by co-polymerization of acrydite-modified DNA or by

reacting amino-modified DNA with hydrogels containing a succinimidyl ester.[75] Since many review papers have already covered these topics,[76,77] we focus here on the physical adsorption of DNA.

4.1. DNA adsorption to hydrogels

To mimic hydrophobic interaction chromatography for the separation of biomolecules, Corman et al. synthesized hydrophobic cryogel disks, which were either plain or particle-embedded.[78] The cryogels were compared for their salmon double-stranded DNA (dsDNA) adsorption efficiency. The authors showed that at higher temperatures, the DNA adsorption capacity increased suggesting that hydrophobic interactions are favourable for DNA adsorption (Fig. 3a). These interactions likely occurred between hydrogel-bound tryptophan, a hydrophobic amino acid used in the hydrogels, and hydrophobic regions of DNA. Moreover, it was shown that the addition of sodium salts increased the adsorption capacity. Polycytosine DNA showed the highest affinity to hydrogels, and similar observations for C-rich DNA were also made on many inorganic nanomaterials and graphene oxide.[79,80]

In another study aimed to separate biological DNA from peas, DNA adsorption was examined on a Co^{2+}-immobilized cryogel.[81] Electrostatic interactions between Co^{2+} ions and the DNA phosphate groups were found to be the dominant mechanism for this adsorption, as increasing temperature and ionic strength reduced the adsorption capacity by disrupting the electrostatic interactions.[81] Furthermore, the adsorption isotherm aligned well with the Langmuir model, suggesting monolayer DNA adsorption.

The Liu group systematically studied the adsorption of short ssDNA on acrylamide-based hydrogels functionalized with boronic acid.[82] Boronic acid was critical for adsorption, as the same hydrogel devoid of boronic acid failed to adsorb the DNA (Fig. 3b). These boronic acid-modified hydrogels were

negatively charged at neutral pH, thereby electrostatically repulsing DNA. Therefore, increasing NaCl concentration promoted DNA adsorption. Moreover, the nanogel could nonspecifically adsorb DNA aptamers and inhibit their binding function. Desorption studies on boronic-acid modified hydrogels suggested that urea and DMSO inhibited DNA adsorption, highlighting the importance of hydrogen bonding and hydrophobic interactions in the DNA adsorption process.[82]

Recently, Huang et al. synthesized a hydrogel containing chitosan and ammonium groups to produce a cationic nanogel for binding and scavenging pathogenic dsDNA in chronic wounds.[83] The nanogel featured quaternary ammonium groups with a high pK_a of ~35, ensuring that it retains a positive charge at the physiological pH of 7.4 and ionic strength of 150 mM, mimicking the chronic wound condition. To confirm the dominance of electrostatic interactions in adsorption, the addition of 1 M NaCl resulted in desorption due to charge screening. The nanogel's structure also played a critical role in DNA scavenging. Smaller DNA molecules (hydrodynamic diameter of 11 nm) penetrated the gel interior, acting as crosslinkers. In contrast, larger genomic DNA (hydrodynamic diameter of 208 nm) primarily adsorbed to the surface. Therefore, fine-tuning the network structure of the hydrogel enabled sequestering of DNA both on the surface and within the interior of the nanogel.

Overall, most acrylamide-based hydrogels do not exhibit strong interactions with DNA oligonucleotides, which explains why DNA can easily retain its hybridization and target-binding functions in such gels. To achieve physisorption of DNA, additional monomers capable of hydrogen bonding, π–π stacking, and electrostatic attraction are needed.

5. Microplastics

Plastics are arguably the most important synthetic polymers. Despite their detrimental environmental effects, plastics are
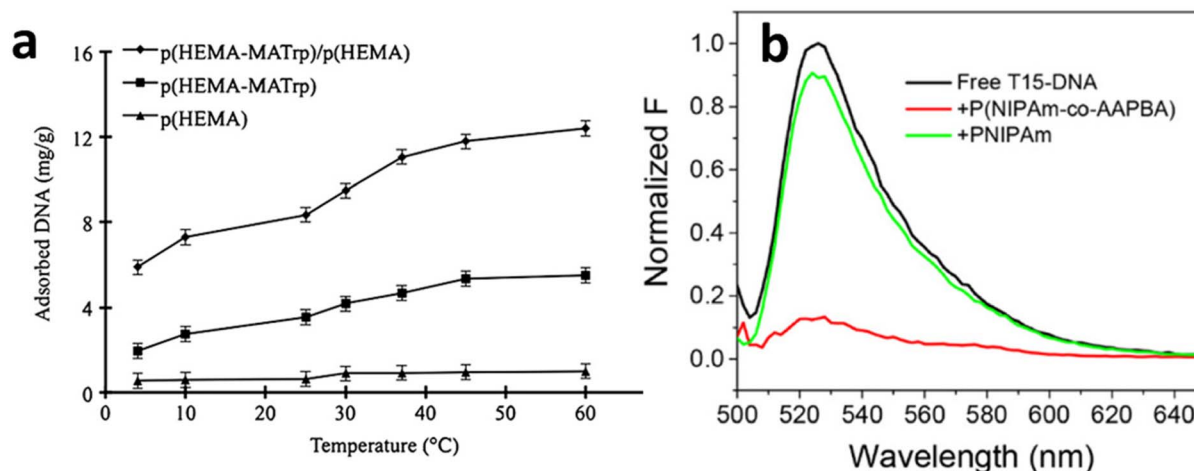

Fig. 3 (a) Effect of temperature on DNA adsorption on tryptophan-containing hydrogels, where increasing temperature enhanced DNA adsorption, suggesting the role of hydrophobic interactions. Reproduced with permission.[78] Copyright 2013, Wiley-VCH. (b) DNA adsorption on acrylamide-based hydrogel with and without boronic acid. Boronic acid was essential for the adsorption of DNA on the hydrogel (red curve). Reproduced with permission.[82] Copyright 2019, American Chemical Society.

still being increasingly produced due to their remarkable versatility and cost-effectiveness. Microplastics are submillimeter plastic particles, which are either intentionally manufactured or generated through the natural shredding of larger plastic objects. The structures of several common microplastics are shown in Fig. 4a. Microplastics are composed of hydrophobic polymer chains, and an important feature is that they are very dense materials with minimal interior water contents, which is distinct from hydrogels.

Studying DNA adsorption to microplastics is important from two aspects. First, it provides fundamental insights into the adsorption of biological DNA to microplastics in the environment. Second, it offers useful information for developing aptamers for microplastics. Some plastics contain aromatic monomers, which may interact more strongly with DNA via π–π stacking interactions. Microplastics can be characterized using optical microscopy to determine their size and shape, and using Raman or IR spectroscopy to analyze composition. Fig. 4b shows a microscope image, and Fig. 4c shows a Raman spectrum of polyethylene terephthalate (PET) microplastics prepared in our lab by grating a plastic water bottle.

5.1. Metal-mediated adsorption

Our group systematically investigated DNA adsorption on microplastics. Since microplastics are negatively charged, we first investigated the effect of environmentally abundant metal ions (Na^+, Mg^{2+} and Ca^{2+}).[84] In the absence of these metal ions, no DNA adsorption was observed. Unlike on PDA, DNA adsorption on microplastics was not dependent on polyvalent metal ions, and Na^+ alone could also induce DNA adsorption on PET microplastics. Similar to PDA, the adsorption affinity to microplastics followed the order $Ca^{2+} > Mg^{2+} > Na^+$, with half-saturation concentrations approximately 85-fold and 4-fold higher for Na^+ and Mg^{2+} compared to Ca^{2+}, respectively (Fig. 5a).

Among the various plastic materials tested,[84] PET and polystyrene (PS) exhibited the highest efficiency for DNA adsorption. These two materials were the only ones with aromatic benzene rings in their chemical structures, suggesting that additional interactions were provided by the aromatic rings. Urea and EDTA both partially induced DNA desorption, indicating the involvement of hydrogen bonding and metal-mediated interactions. Moreover, a surfactant (Tween 80) fully desorbed DNA, which was attributed to the hydrophobic tail of Tween 80 interacting with the plastic surface via van der Waals (VDW) forces, thereby displacing the DNA.

5.2. Adsorption of biological DNA

Salmon sperm DNA ($\sim$2000 bp) was used to investigate dsDNA to microplastics.[85] Although metal ions were critical for the adsorption of ssDNA to microplastics, this DNA adsorbed even in the absence of metal ions (Fig. 5b). However, shorter dsDNA (24-mer), matching ssDNA length, did not adsorb without metal ions.[85] These findings suggested that polyvalent binding, enabled by numerous binding sites on long biological DNA, likely enhanced weak individual interactions. The effect of transition metal ions (including Mn^{2+} and Zn^{2+}) was then examined and they resulted in higher adsorption affinity compared to Mg^{2+} (Fig. 5c).[85] Furthermore, the use of transition metal ions resulted in DNA adsorption on certain plastic materials, such as polyvinyl
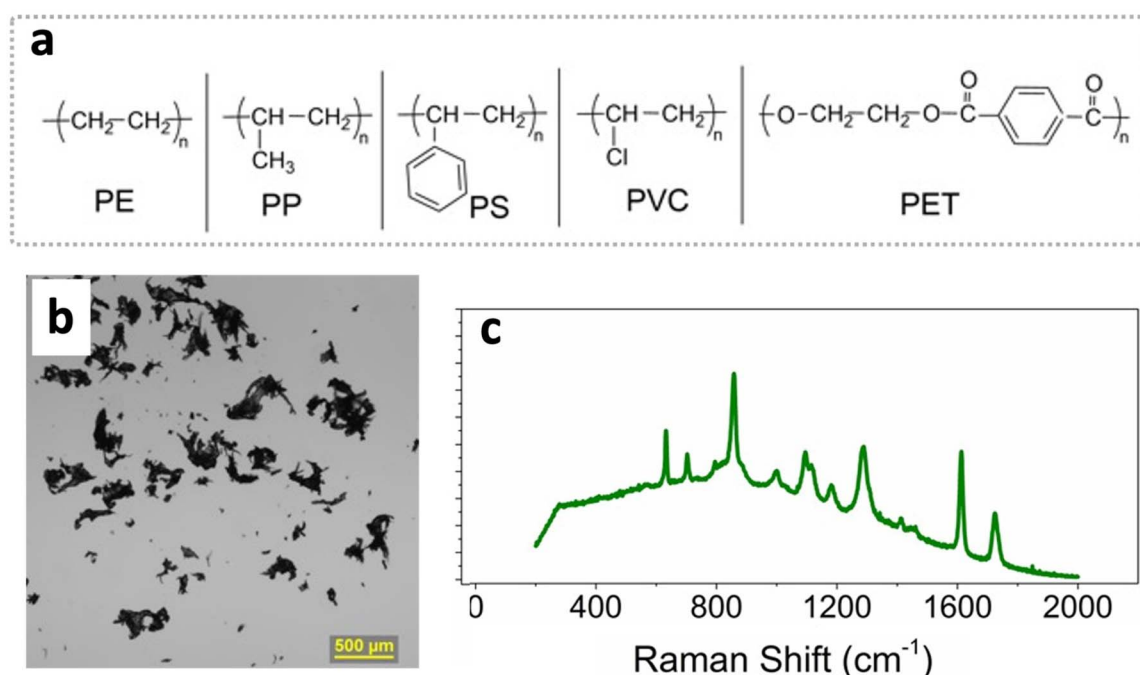

Fig. 4 (a) Molecular structures of common plastic materials. (b) An optical micrograph and (c) a Raman spectrum of PET microplastics generated in our lab by grating a plastic water bottle. Reproduced with permission.[84] Copyright 2022, American Chemical Society.
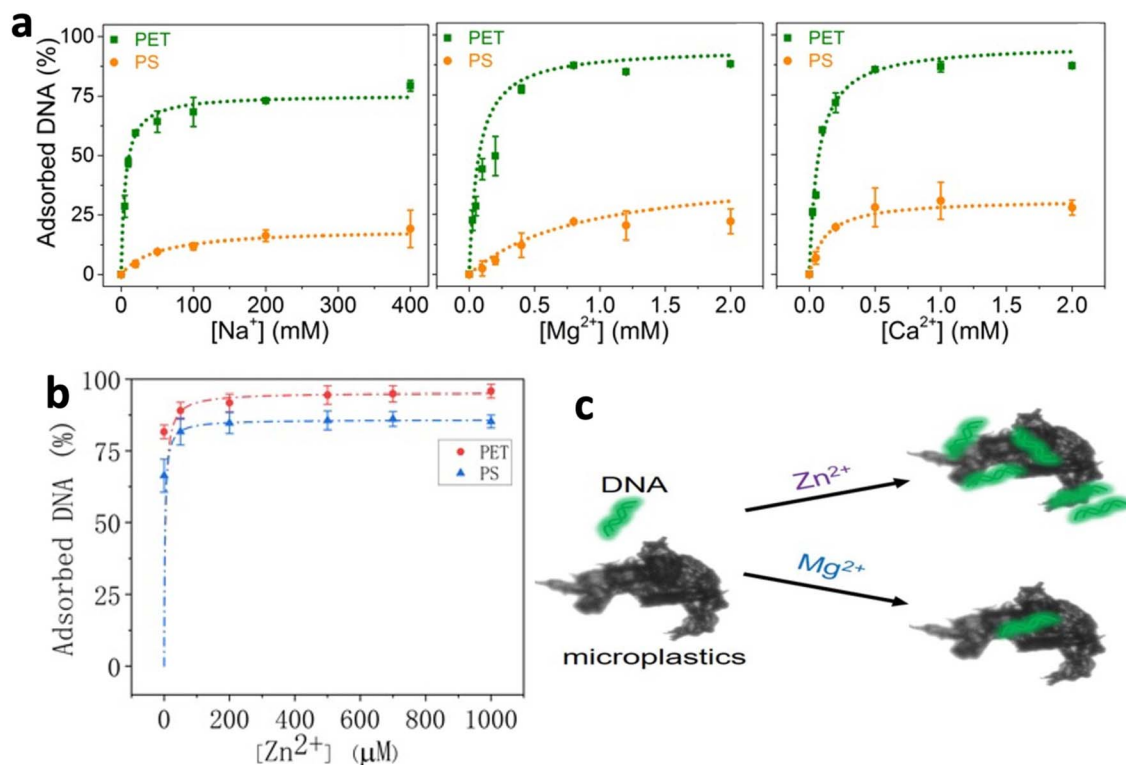
Fig. 5 (a) Adsorption of FAM-DNA (10 nM) onto PET and PS microplastics (50 μg mL^{-1}) in the presence of increasing concentrations of Na$^+$, Mg^{2+}, or Ca^{2+}. Reproduced with permission.[84] Copyright 2022, American Chemical Society. (b) Adsorption of salmon dsDNA (~2000 bp, 1 μM DNA base concentration) onto PS and PET microplastics (500 μg mL^{-1}) in 10 mM HEPES buffer (pH 7.6) in the presence of increasing Zn^{2+} concentrations. (c) A scheme suggesting the higher efficiency of transition metal ions (such as Zn^{2+}) compared to alkaline earth metal ions (such as Mg^{2+}) for DNA adsorption onto microplastics. Panels b and c were reproduced under the terms of the CC-BY Creative Commons Attribution 4.0 International license (https://www.creativecommons.org/licenses/by/4.0).[85]

chloride (PVC), which did not adsorb DNA in the presence of alkali or alkaline earth metal ions (Na$^+$, Mg^{2+} and Ca^{2+}).

Moreover, our group has shown that the wettability of microplastics affected the adsorption efficiency to SNA.[86] Enhanced wettability provided a larger surface area for adsorption. Therefore, more careful standardization of microplastics surfaces is necessary, and time-dependent changes in microplastics needs to be considered in adsorption studies.

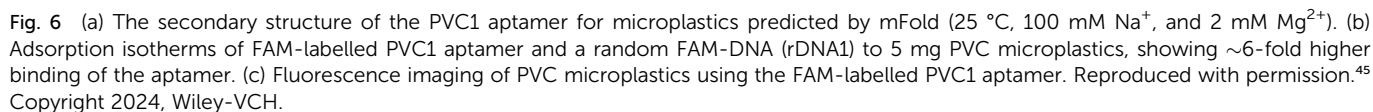### 5.3. Selection of DNA aptamers for microplastics

After understanding the adsorption affinity of DNA to various microplastics, we believe it should be feasible to select aptamers for certain microplastics, such as PS and PVC. PET, in contrast, adsorbs DNA too strongly, and aptamer selection may not be feasible. Using a DNA library containing 30 random nucleotides, we used both PS and PVC microplastic as targets for aptamer selection. Interestingly, both selections yielded the same aptamer sequence featured with a C/T-rich loop without an obvious internal secondary structure (Fig. 6a),[45] which allows maximal contact with the plastic surface. Although each C and T nucleotide is expected to adsorb less strongly than A and G, polyvalent interactions from multiple C/T adsorption sites can still be quite strong. Molecular dynamics simulations also supported this hypothesis. We believe this sequence may serve as a general aptamer for many types of plastics.

The aptamer binds to PVC and PS microplastics with high affinity, showing a six-fold higher binding capacity than random DNA (Fig. 6b). Its binding capacity was significantly higher for PVC and PS compared to other plastics, such as polyethylene (PE) (Fig. 6C). Additionally, the aptamer's ability to distinguish between plastic and non-plastic materials, such as silica, was demonstrated through fluorescence-based detection (Fig. 6c).

6. Cellulose

Cellulose is a naturally abundant biopolymer found in the cell walls of plants, algae, and some bacteria. Cellulose crystals, encompassing cellulose microcrystals (CMC) and cellulose nanocrystals (CNC), represent highly ordered forms of this polysaccharide, characterized by exceptional mechanical strength and high surface area, and can be functionalized with a variety of surface molecules.[87] At the nanoscale, CNCs are typically 5–20 nm in width and 100–500 nm in length, and they possess higher hydrophilicity, chemical reactivity, and adsorption capacity compared to CMC.[88] Their biocompatibility, biodegradability, and renewable sourcing further enhance their appeal for applications at biointerfaces, such as drug delivery systems, tissue engineering scaffolds, biosensors, and environmental remediation platforms.[89] The tunable surface

Fig. 6 (a) The secondary structure of the PVC1 aptamer for microplastics predicted by mFold (25 °C, 100 mM Na$^+$, and 2 mM Mg^{2+}). (b) Adsorption isotherms of FAM-labelled PVC1 aptamer and a random FAM-DNA (rDNA1) to 5 mg PVC microplastics, showing ~6-fold higher binding of the aptamer. (c) Fluorescence imaging of PVC microplastics using the FAM-labelled PVC1 aptamer. Reproduced with permission.[45] Copyright 2024, Wiley-VCH.

chemistry of cellulose crystals, achievable through methods like oxidation, esterification, or grafting, allows precise control over their functionality.[90,91] The surface of cellulose is rich in hydroxyl (–OH) groups, and depending on the preparation method (e.g., sulfuric acid hydrolysis for nanocellulose), may also contain sulfonate (–SO$_3^-$) groups (Fig. 7a). So, DNA generally does not exhibit strong interactions with cellulose.

6.1. DNA adsorption on cellulose

One of the most important applications of cellulose is in the paper industry. To develop paper surfaces for pathogen detection, Su *et al.* investigated DNA adsorption and covalent coupling of DNA on CMC.[92] The ATP DNA aptamer was used as a model DNA in this study. It was shown that physical adsorption was weak and reversible. In contrast, covalent coupling of an amine-modified aptamer to cellulose through a Schiff-base reaction resulted in highly stable conjugates, while the aptamer retained its specificity for ATP detection. Since the
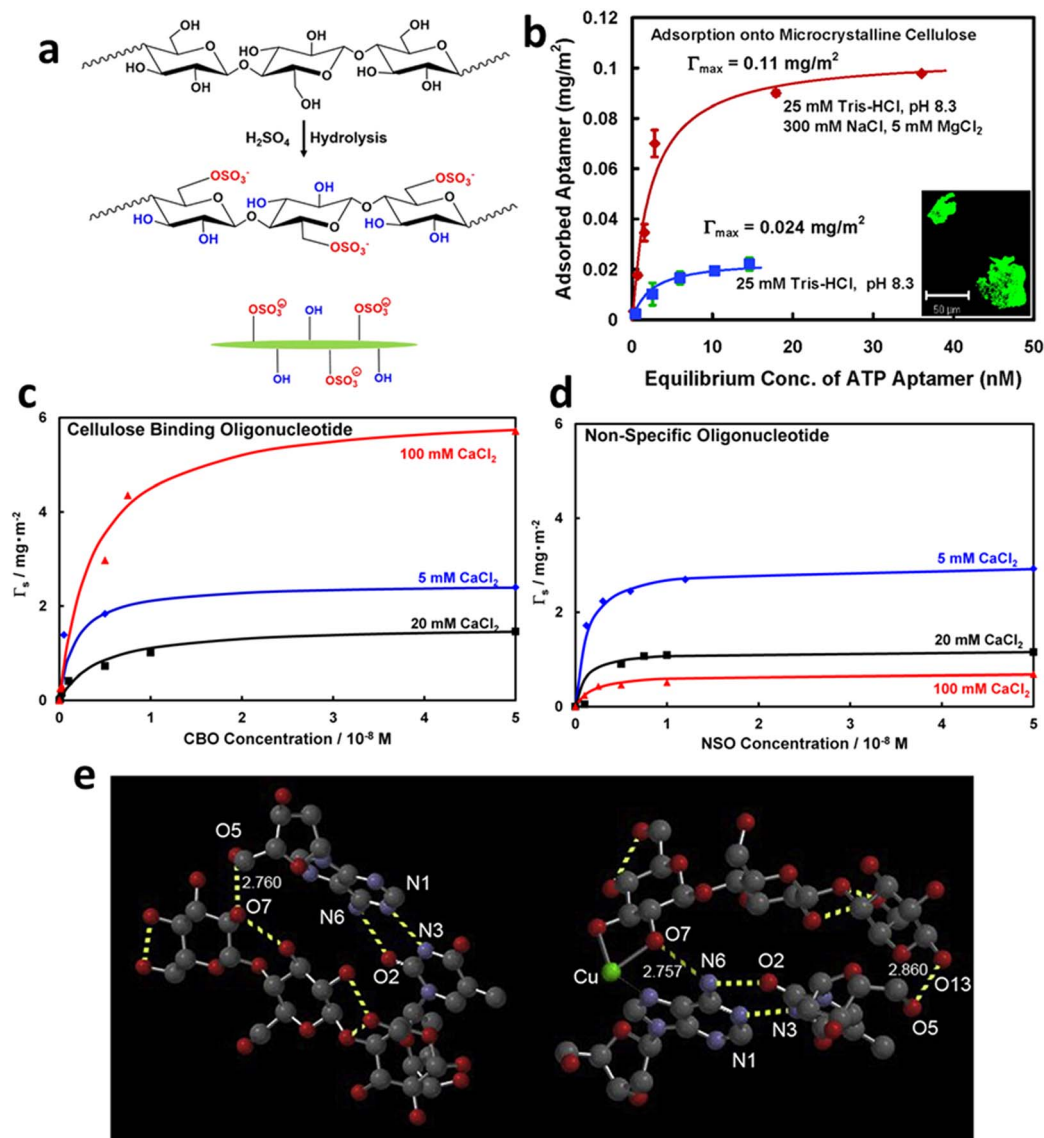
CMC was slightly negatively charged, with increasing ionic strength (300 mM NaCl and 5 mM MgCl$_2$), electrostatic repulsion was reduced and DNA adsorption increased (Fig. 7b). When the adsorbed DNA was washed with buffer devoid of metal salts, DNA was consistently desorbed from the surface, suggesting very weak adsorption that was highly dependent on ionic strength.[92]

Sato *et al.* investigated the adsorption of a previously reported cellulose-binding (CB) DNA aptamer on various types of CNCs and compared it with the adsorption of a random DNA sequence (rDNA). A much higher adsorption capacity of the CB DNA was observed, particularly at high concentrations of Ca^{2+} ions.[93] Upon increasing the Ca^{2+} concentration from 20 mM to 100 mM, the adsorption of the CB DNA increased significantly, whereas the adsorption of the rDNA was conversely inhibited (Fig. 7c and d). The authors suggested that at a high Ca^{2+} concentration of 100 mM, the CB aptamer likely adopts its favourable binding conformation. In contrast, nonspecific adsorption of DNA is related to hydrogen bonding and Ca^{2+}-

Fig. 7 (a) Typical chemical composition of a pristine cellulose polymer, modified cellulose incorporating sulfonate moieties, and CNC featuring both neutral hydroxyl and negatively charged sulfonate surface groups. Reproduced under the terms of the CC-BY Creative Commons Attribution 4.0 International license (https://www.creativecommons.org/licenses/by/4.0).[95] (b) Adsorption isotherms for the adsorption of the ATP aptamer to CMC in different buffer conditions, and both curves were fitted to the Langmuir model, Inset: a confocal micrograph depicting fluorescent CMC after adsorption of the fluorophore-labelled ATP aptamer. Reproduced with permission.[92] Copyright 2007, American Chemical Society. (c and d) Effect of increasing Ca^{2+} concentration on the selective adsorption of the CB DNA aptamer over a random DNA. With 100 mM Ca^{2+}, the CB DNA adsorption remarkably increased, while the adsorption of the rDNA was inhibited. Reproduced with permission.[93] Copyright 2012, American Chemical Society. (e) Simulation results revealing that A/T nucleotides adsorb to cellulose via hydrogen bonding (left), while Cu^{2+} enables additional adsorption through metal coordination (right). Reproduced with permission.[94] Copyright 2017, Elsevier B.V.

mediated bridging interactions. Beyond a critical salt concentration, such as 100 mM $CaCl_2$, the high ionic strength saturated the system with counterions, reducing the likelihood of Ca^{2+} forming bridging interactions. Instead, Ca^{2+} ions neutralized the charges on DNA and the cellulose surface, decreasing their mutual attraction.[93] Additionally, the CB DNA aptamer was grafted to polyacrylamide to facilitate its adsorption onto CNCs.

Mujtaba et al. used a Cu^{2+}-immobilized cellulose surface to adsorb a plasmid DNA.[94] The Cu-modified cellulose adsorbed

~50% more of the plasmid DNA than bare cellulose. Since cellulose is negatively charged at neutral pH, metal ions were added to reduce the charge repulsion. The authors further used quantum calculation to analyse the electrostatic and chemical interactions between DNA and cellulose, which revealed that hydrogen bonding stabilized Cu^{2+} ions on the cellulose surface (Fig. 7e).[94] Their mechanistic analyses indicated that the adsorption of DNA on cellulose involves both hydrogen bonding and hydrophobic interactions. Hydrogen bonds form between

the hydroxyl groups of cellulose and the proton donor (NH_2) and acceptor (C=O) groups of DNA bases, while hydrophobic interactions arise from the aromatic rings of DNA bases and the hydrophobic regions of cellulose. The binding is further influenced by metal ions such as Cu^{2+}, which can coordinate with specific DNA sites and further stabilize the interaction.

6.2. Selection of aptamers for cellulose

The Breaker group selected both DNA and RNA aptamers for cellulose.[96,97] The DNA aptamer named CELAPT 14 exhibited robust binding to cellulose powder and paper, enabling applications related to DNA immobilization on cellulose-based materials.[96] The aptamer's binding was strong enough to remain functional even in the presence of detergents like SDS, which typically disrupt non-specific adsorption. The aptamer's secondary structure was analysed (Fig. 8a), revealing a complex architecture with conserved G-rich regions that may form a G-quadruplex structure. In comparison, the DNA aptamer for microplastics (PVC-1) selected by our group was pyrimidine-rich (~90% cytosine and thymine).[45] In addition, the PVC-1 aptamer features a C/T-rich loop without obvious internal secondary structure (Fig. 6a), allowing maximal contact with the plastic surface through polyvalent interactions. Both aptamers demonstrate high specificity for their targets. However, the cellulose aptamer relies on structured G-quadruplexes, whereas the microplastic aptamer achieves binding through flexible, unstructured loops, highlighting different strategies for surface-binding aptamers.

An optimized RNA aptamers for cellulose named 4–15 was also reported by the Breaker group, which binds robustly to cellulose in both powder and paper forms.[97] The aptamer's binding also remained functional in SDS-containing buffers, and structural analysis revealed conserved stem-loop motifs

essential for activity (Fig. 8b). Unlike the G-quadruplex-dependent DNA cellulose aptamer (CELAPT 14),[96] the RNA aptamer relies on a distinct secondary structure without a G-rich motif. It was fused to a glmS ribozyme and achieved affinity-based RNA purification. These findings highlight divergent structural strategies—structured stems in RNA *versus* G-quadruplexes in DNA—for achieving high-affinity cellulose binding.

7. Nanodiamonds (NDs)

While extensive studies have been carried out on interfacing DNA with carbon nanotubes and graphene oxide, studies on NDs remain relatively limited. NDs have emerged as a unique quantum material whose quantum effect can be measured under ambient conditions. NDs typically ranging from 5 to 100 nm, contain a crystalline diamond core. Their quantum effects are originated from their appealing nitrogen-vacancy (NV) centers, which are atomic defects within the diamond lattice where a nitrogen atom replaces a carbon atom adjacent to a vacancy. These NV centers endow NDs with remarkable fluorescence properties, emitting stable, bright light across a broad spectrum, particularly in the red and near-infrared range, without photobleaching or photoblinking. NV centers in NDs also exhibit quantum properties, including spin coherence and sensitivity to external stimuli such as magnetic and electric fields. Furthermore, the surface of NDs can be readily modified with a diverse array of functional groups, such as carboxyl, hydroxyl, and amine groups.

7.1. DNA adsorption on NDs

To conjugate DNA oligonucleotides to NDs, coating NDs with polymers has been widely used. Zhang *et al.* coated NDs with
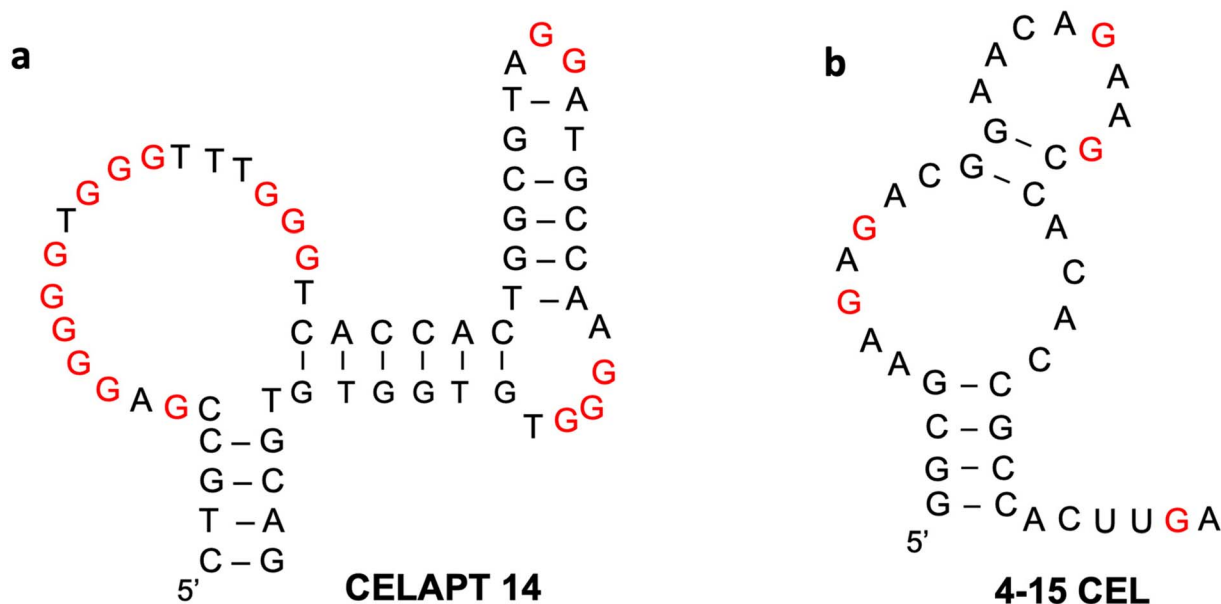

Fig. 8 (a) The secondary structure of the CELAPT 14 DNA aptamer containing a few G-rich regions.[96] (b) The secondary structure of the 4–15 cellulose RNA aptamer, which lacks G-rich regions.[97]
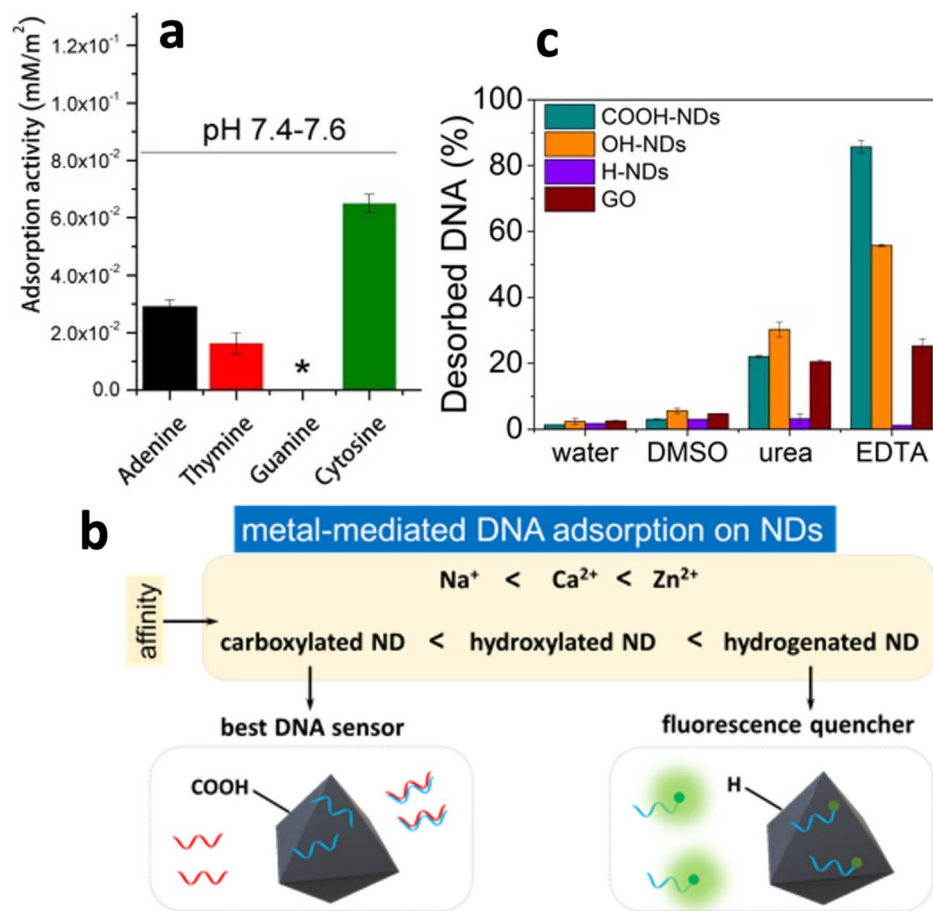
Fig. 9 (a) Adsorption efficiency of different DNA nucleobases on NDs at pH ~7.5. Reproduced with permission.[99] Copyright 2018, American Chemical Society. (b) A scheme depicting the effect of various metal ions and surface functional groups on the efficiency of DNA adsorption on NDs.[100] (c) DNA desorption from NDs and GO induced by 50% DMSO, 4 M urea, or 10 mM EDTA in a buffer solution containing 200 μM Ca^{2+} (10 mM HEPES, pH 7.6) suggesting the order of adsorption affinity. Reproduced with permission.[100] Copyright 2023, American Chemical Society.

a positively charged polymer, PEI, to provide electrostatic attraction for the adsorption of plasmid DNA.[98] Laptinskiy *et al.* investigated the adsorption of different DNA nucleobases to carboxyl-modified NDs both experimentally and *via* simulations.[99] The experimental studies revealed that for individual nucleobase adsorption, the order of adsorption activity on COOH-NDs at neutral pH was cytosine > adenine > thymine (Fig. 9a). Since uncharged DNA nucleobases were used, no metal ions were needed. Molecular dynamics modelling suggested that hydrogen bonding to carboxylic groups was important for the physical adsorption.[99]

Recently, our group systematically investigated the adsorption of DNA oligonucleotides to carboxylated (COOH–), hydroxylated (OH–), and hydrogenated (H–) NDs.[100] We tested the effect of several common metal ions. In the presence of Na^+, the order of adsorption affinity followed the trend H– > OH– > COOH– (Fig. 9b). Only the hydrogenated NDs exhibited fluorescence quenching property, likely due to their exceptional electron transfer capability, which facilitated the Dexter electron transfer based quenching mechanism.[101] To further explore the nature of DNA interaction with NDs, DNA desorption studies were conducted.[100] Urea as a hydrogen bonding disruptor, induced some

desorption, suggesting the involvement of hydrogen bonding in DNA adsorption. When adsorption was promoted by Ca^{2+}, EDTA also induce DNA desorption from NDs in the order of COOH– > OH– > H–, where almost all DNA desorbed from the COOH-NDs, while no desorption occurred from the H-NDs (Fig. 9c). This study reflected the order of adsorption affinity to the NDs and suggested that metal-mediated interactions were the dominant mechanism. The lack of desorption from H-NDs indicated an extraordinarily DNA adsorption affinity.

8. Carbon quantum dots (CQDs)

CQDs are fluorescent carbon-based NPs with sizes typically below 10 nm, known for their excellent biocompatibility and optical properties. Their surface chemistry, characterized by functional groups like carboxyl and amine groups, plays a key role in their solubility, stability, and ability to be chemically modified for specific applications (Fig. 10a).[102,103] CQDs are synthesized from various starting materials using methods such as electrochemical carbonization, hydrothermal treatment, microwave-assisted synthesis, or laser ablation, which allow control over their size and surface properties.[104] However, due to their extremely small
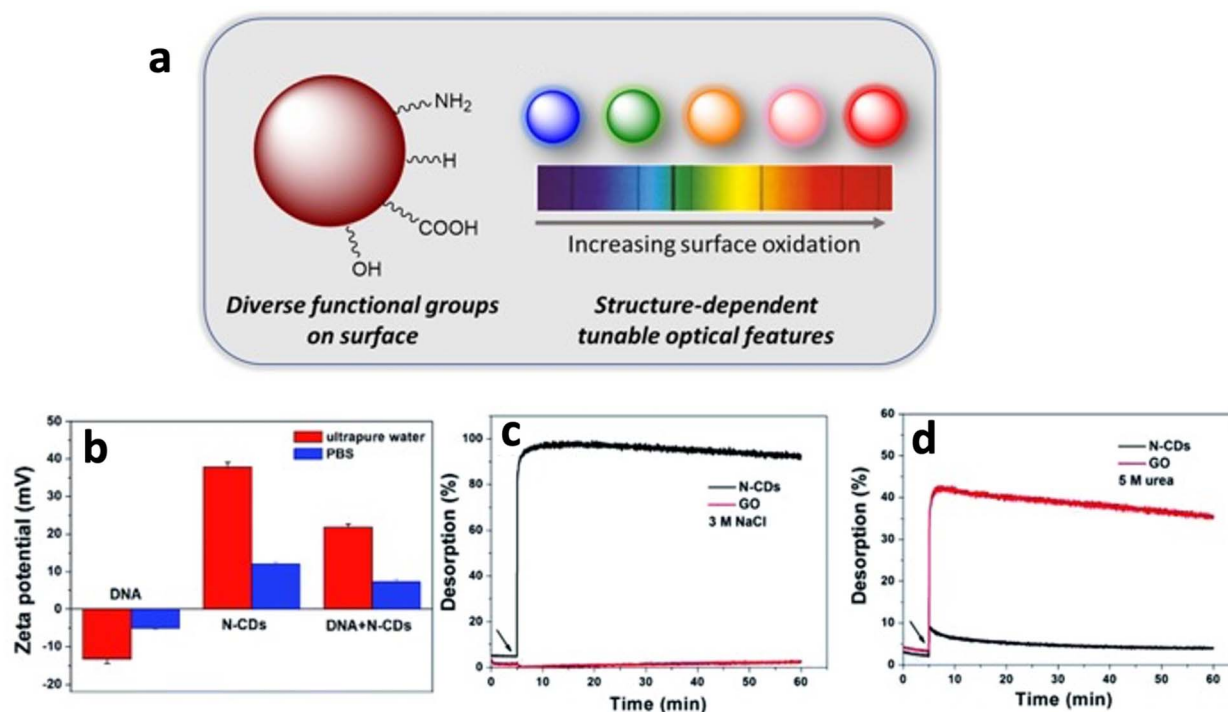
Fig. 10 (a) A scheme showing the typical surface functional groups of CQDs and their oxidation-dependent photoluminescence characteristics. Reproduced under the terms of the CC-BY Creative Commons Attribution 4.0 International license (https://www.creativecommons.org/licenses/by/4.0).[103] (b) ζ-potentials of DNA, nitrogen-doped CQDs, and their mixtures in ultrapure water *versus* PBS (10 mM, pH 7.4). Nitrogen doping altered the surface charge of CQDs.[106] Comparison of DNA desorption from GO *versus* CQDs induced by (c) 3 M NaCl, (d) 5 M urea. Reproduced with permission.[106] Copyright 2019, Royal Society of Chemistry.

size, most CQDs cannot be easily precipitated by centrifugation, requiring alternative separation techniques such as dialysis or filtration for purification.[105]

8.1. DNA adsorption on CQDs

Li *et al.* used nitrogen doping to alter the surface charge of CQDs to positive to achieve electrostatically-mediated DNA adsorption, and the positive charge of the CQDs was confirmed by zeta potential measurements (Fig. 10b).[106] Graphene oxide (GO) was used as another carbon-based nanomaterial for benchmark. The addition of NaCl induced 100% desorption of DNA oligonucleotides from the positively charged nitrogen-doped CQDs, suggesting the predominant role of electrostatic attraction in DNA adsorption (Fig. 10c).[106] Moreover, the addition of inorganic phosphate and adenosine both resulted in partial desorption, suggesting that DNA used both the phosphate backbone and nucleobases for adsorption. Urea-induced desorption from CQDs was significantly less than from GO, indicating a smaller role of hydrogen bonding (Fig. 10d). Furthermore, two ionic surfactants (CTAB and SDS) induced significant desorption form CQDs compared to GO, which suggested the involvement of van der Waals forces, hydrophobic interactions, or the weakening of electrostatic interactions in DNA adsorption on the positively charged CDs.

Han *et al.* demonstrated the adsorption of long biological dsDNA and single-stranded RNA (ssRNA) on cell-penetrating CQDs.[107] They modified CQDs with triphenylphosphine, which provided a positively charged surface (approximately +20 mV) that facilitated the adsorption of negatively charged nucleic acids. They hypothesized that electrostatic and π–π interactions, as well as hydrogen bonding, were important for adsorption. Their data suggested that the rigid structure of dsDNA traps CQDs within its grooves, enhancing the fluorescence by confining the intramolecular rotation of the CQDs. In contrast, ssRNA, due to its flexibility, clusters CQDs together into close contact.

9. Applications of DNA-functionalized materials

DNA-functionalized inorganic nanomaterials have been at the forefront of the bionanotechnology field. The most classical example is probably SNAs,[61] which were initially developed using a AuNP core densely coated with a layer of DNA. Later, this concept was extended to other types of core materials, which also exhibited intriguing physicochemical properties. Nevertheless, the use of metal-free materials to interface with DNA has attracted growing interest. In this section, we briefly describe a few of representative applications.

9.1. Signal-on biosensors

PDA, crystalline cellulose, CQDs, and some NDs act as fluorescence quenchers, which facilitates the construction of signal-on
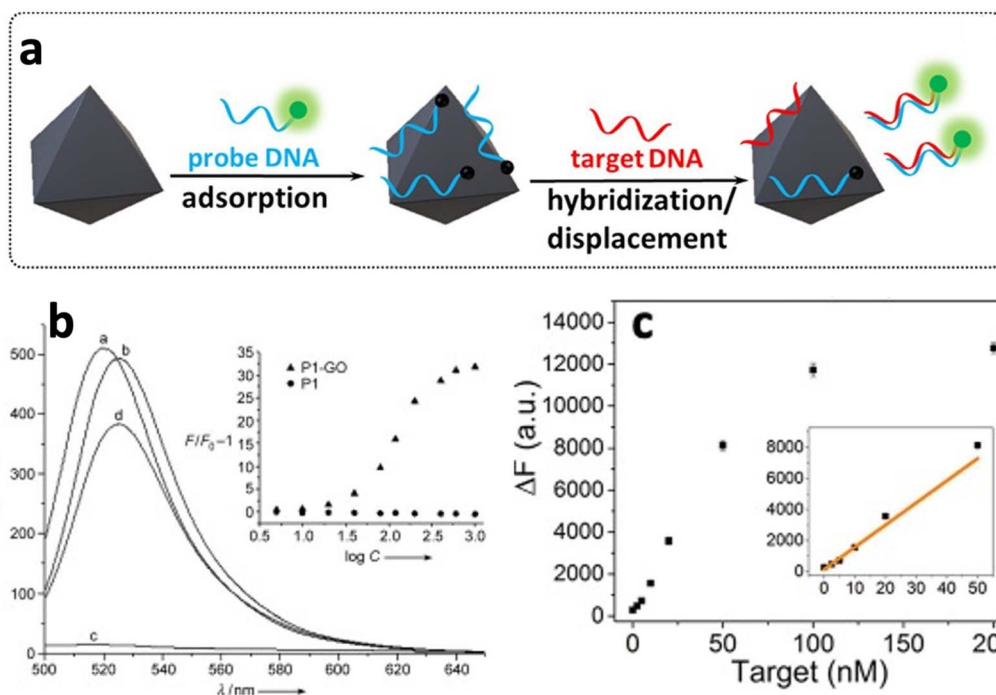
Fig. 11 (a) A scheme depicting the principle of a DNA hybridization–based signal–on biosensor. Reproduced with permission.[100] Copyright 2023, American Chemical Society. (b) Fluorescence signal enhancement of (b) GO–based, and (c) PDA–based biosensors when used for the detection of various concentrations of target cDNA. Panel b is reproduced with permission.[108] Copyright 2009, Wiley-VCH. Panel c is reproduced with permission.[54] Copyright 2021, American Chemical Society.

biosensors based on the adsorption of fluorophore-labelled DNA oligonucleotides. In a typical sensor design (Fig. 11a), a fluorophore-labelled probe DNA is adsorbed onto the surface of these nanomaterials, resulting in quenching and decrease in fluorescence signal. When a complementary target DNA is introduced, it hybridizes to the probe, and the resulting dsDNA is desorbed from the surface, leading to an enhancement of the fluorescence signal. The best-known example is to use GO as initially reported by Yang and coworkers. The fluorescence increase ($[F - F_0]/F_0$) upon adding cDNA reached up to 30-fold (Fig. 11b).[108] Using PDA in place of GO, we achieved a 12-fold fluorescence enhancement (Fig. 11c),[54] whereas COOH-NDs demonstrated $\sim$25-fold signal enhancement.[100] Aside from a high signal-to-background ratio, these new materials may possess other advantages, such as intrinsic fluorescence, which may allow the use of non-labelled DNA. Biocompatibility is another advantage. For example, PDA is made of biomolecules and may offer superior biocompatibility, making it useful for intracellular detection. Our group has applied DNA adsorption on NDs for DNA detection. It was suggested that sensor performance followed the order of COOH– > OH– > H– for the surface groups on NDs, which was inversely correlated to adsorption affinity (Fig. 9b).[100] Therefore, tighter adsorption resulted in lower signaling, with H-NDs being unable to differentiate between the target DNA and a random DNA.

Loo *et al.* adsorbed DNA oligonucleotides to two carboxylic acid-functionalized CQDs (citric acid and malic acid as starting materials) to design sensors for DNA detection. The malic acid

CQDs exhibited superior quenching efficiency (39% *vs.* 23%) attributable to their higher carboxylic group density. They achieved detection ranges of 0.4–400 nM (citric acid) and 0.04–400 nM (malic acid), with limits of detection of 45.6 nM and 17.4 nM, respectively. Furthermore, selectivity for single-base mismatches was demonstrated.[109]

Wei *et al.* adsorbed ssDNA to CQDs for the detection of acrylamide.[110] In the absence of the target, a ssDNA adsorbed to CQDs through interactions with amino and carboxylic acid groups. The authors did not use an aptamer for acrylamide and relied on nonspecific interactions. In the presence of acrylamide, it binds to the DNA *via* hydrogen bonding to the oxygen and nitrogen atoms of DNA nucleobases. As a result, ssDNA adsorption is partially inhibited, leading to an increase in fluorescence signal. Our group recently selected DNA aptamers for acrylamide, which only achieved a K_d of 4.7 mM.[111] Considering such weak interactions between the aptamer and acrylamide, another possibility is that acrylamide interacted with CQDs, which weakened the adsorption of the DNA.

9.2. DNA extraction

DNA extraction is critical for various biotechnological and analytical applications. The Jia group utilized the pH-switchable surface of PDA to achieve DNA extraction.[49,50] They demonstrated that efficient DNA adsorption could be achieved at pH 2, and that increasing the pH to 8 induced charge repulsion, resulting in the release of the captured DNA. The group used the adhesive properties of PDA to synthesize PDA-coated magnetic
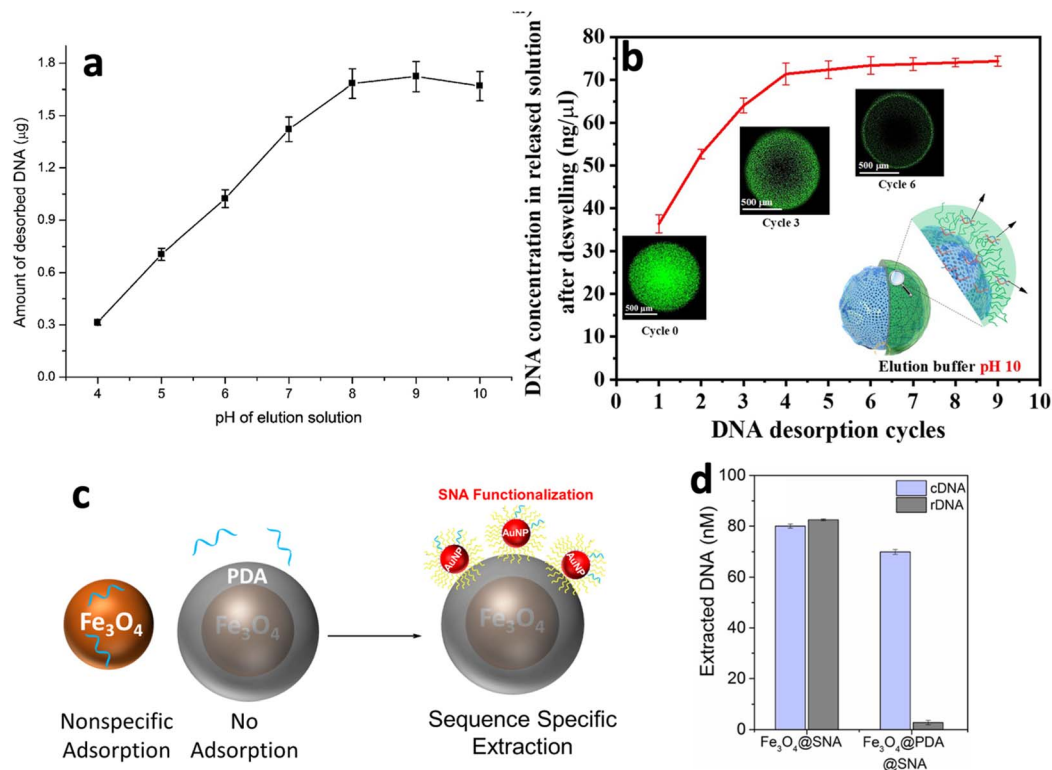
Fig. 12 (a) Effect of pH on the desorption/elution of DNA from a PDA-coated microtube surface. Reproduced with permission.[50] Copyright 2017, Elsevier B.V. (b) Elution of DNA at high pH from a pH-responsive PEI-containing hydrogel after multiple cycles. Reproduced under the terms of the CC-BY Creative Commons Attribution 4.0 International license (https://www.creativecommons.org/licenses/by/4.0).[112] (c) A scheme depicting a hybrid PDA structure for sequence-specific extraction of DNA. PDA does not adsorb ssDNA in Na$^+$-containing buffer, thereby inhibiting the adsorption of rDNA. The probe SNA hybridizes with the target cDNA.[114] (d) Sequence specific extraction of cDNA compared to the absence of PDA, where rDNA nonspecifically adsorbs onto magnetic NPs. Reproduced with permission.[114] Copyright 2021, American Chemical Society.

NPs and PDA-coated microtubes, which achieved high DNA adsorption capacities of 161 mg g^{-1} and 81% elution efficiency, respectively (Fig. 12a).

Fei *et al.* synthesized a dual-responsive hydrogel that exhibits both thermal and pH responsiveness by incorporating *N*-isopropylacrylamide (NIPAM) and polyethylenimine (PEI), respectively.[112] NIPAM provides thermoresponsiveness with a lower critical solution temperature of $\sim$32 °C, enabling reversible swelling and deswelling for DNA encapsulation. At pH 5 and a temperature of 20 °C, the dried hydrogel beads swelled in the DNA solution, enabling DNA uptake due to electrostatic attraction between the protonated amine groups of PEI and the negatively charged DNA molecules.[112] In contrast, at a high pH of 9, deprotonation of the amine groups resulted in the release of DNA from the hydrogel (Fig. 12b). Moreover, Zhang *et al.* used cellulose-functionalized superparamagnetic beads for the isolation and extraction of biological DNA.[113] The DNA adsorption followed the Langmuir isotherm, although the mechanism of adsorption was not discussed.

In a different approach, our group has achieved sequence-specific DNA extraction by developing a hybrid magnetic nanoparticle.[114] In this approach, Fe$_3$O$_4$ NPs were coated with PDA, and subsequently functionalized with SNAs to provide a high density of probe DNA (Fig. 12c). PDA did not adsorb DNA

at neutral pH without divalent metal ions, and therefore nonspecific DNA extraction was inhibited. The SNA-modified PDA NPs enabled fast and effective DNA extraction attributable to a favourable upright conformation of the probe DNA strands on SNA (Fig. 12d).

9.3. Hydrogels for DNA storage

Using DNA to convert digital information is an emerging research direction that has attracted significant attention recently.[115] DNA extraction and storage are closely intertwined processes, as the methods used for extraction often influence the suitability of DNA for long-term storage. As mentioned in the DNA extraction section above, Fei *et al.* employed responsive hydrogels for DNA extraction, which also enabled high-density and long-term storage of information.[112] A cationic polymer (PEI) was modified onto a negatively charged hydrogel matrix to facilitate DNA extraction, while the thermoresponsive hydrogel allowed multiple swelling and deswelling cycles. As a result, a DNA storage density of up to 7 × 10^9 GB g^{-1} was achieved, as the hydrogel could concentrate DNA through repeated cycles until saturation.

Similarly, Ding *et al.* developed bio-informational hydrogel microspheres for the extraction and storage of cell-free DNA (cfDNA) using PDA nanosheets (PDA NSs) encapsulated within
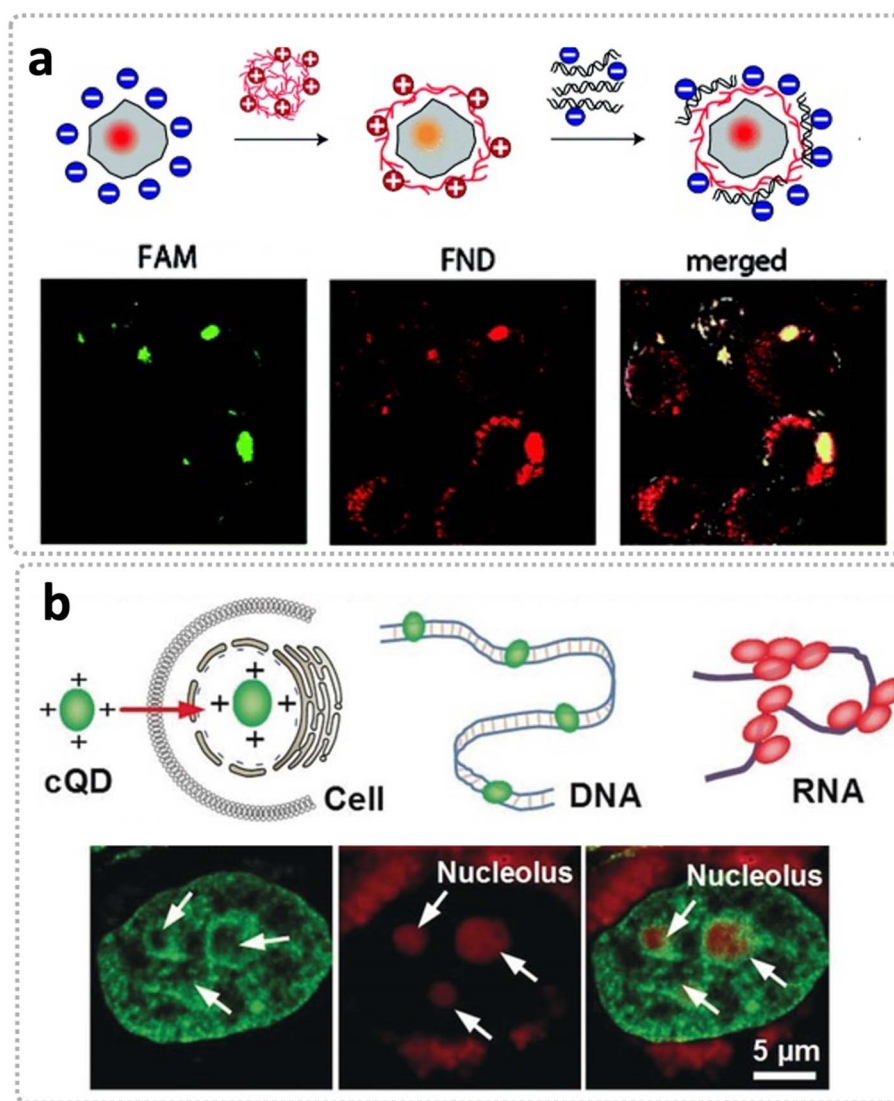
Fig. 13 (a) Intracellular delivery of FAM–DNA adsorbed onto the ND surface. The NDs were coated with positively charged PEI. The red fluorescence resulted from the intrinsic fluorescence of the NDs. Reproduced with permission.[117] Copyright 2016, Royal Society of Chemistry. (b) Intracellular delivery of CQDs adsorbed onto nucleic acids: DNA (green fluorescence) and RNA (red fluorescence). Reproduced with permission.107 Copyright 2019, Wiley-VCH.

gelatin-methacryloyl hydrogel microspheres.[116] The π–π stacking and hydrogen bonding interactions between PDA NSs and cfDNA enabled efficient DNA capture, while the hydrogel's polymer network provided a cage-like spatial confinement for DNA storage. This system not only demonstrated a high cfDNA binding efficiency but also reduced chronic inflammation by blocking cfDNA-mediated pro-inflammatory signaling pathways. Therefore, the versatility of the PDA/hydrogel material was demonstrated for both information storage and biomedical applications.

9.4. Intracellular delivery and imaging

Zhang *et al.* coated the surface of NDs with PEI to facilitate the adsorption of plasmid DNA.[98] In addition, PEI can interact with cell membranes, promoting endocytosis and facilitating cellular

entry. Therefore, this system was used for gene delivery. Petrakova *et al.* used the same PEI coating method for electrostatic adsorption of DNA and its delivery into cells (Fig. 13a).[117] Reversible adsorption of DNA to NDs facilitated intracellular release. Moreover, the release process was monitored *via* nitrogen vacancy colour centres and its intrinsic fluorescence (Fig. 13a).

Han *et al.* developed an imaging probe using photostability of CQDs that can penetrate biological membranes. The CQDs were positively charged and capable of adsorbing and mapping dsDNA and ssRNA.[107] The more rigid dsDNA enhanced the green fluorescence signal by trapping CQDs in the grooves, whereas the flexible ssRNA promoted clustering of CQDs resulting a red fluorescence emission (Fig. 13b).

Qiang *et al.* utilized PDA–DNA conjugates for intracellular ATP detection.[118] PDA protected the adsorbed aptamer probe from enzymatic degradation, enabling selective ATP sensing in
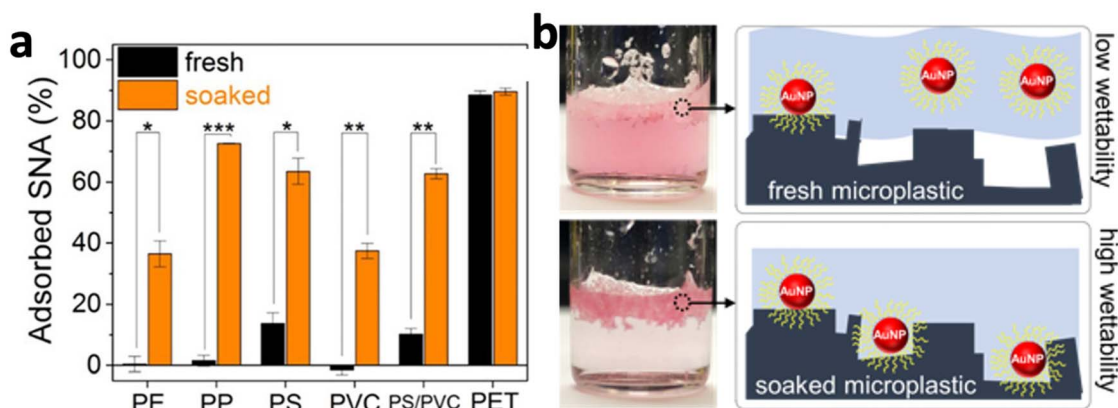
Fig. 14 (a) Enhanced SNA adsorption on various soaked microplastics. (b) Photographs showing enhanced SNA adsorption on soaked PP microplastics and a schematic illustration depicting the effect of wettability on SNA adsorption efficiency. Reproduced with permission.[86] Copyright 2023, American Chemical Society.

HeLa cells. Similarly, Choi *et al.* designed AuNP@PDA nanoprobes for miRNA detection in hMSCs, achieving higher cellular uptake compared to commercial probes.[119] He *et al.* further developed a ZnO@PDA system for tumor mRNA imaging, where dissolution of intracellular ZnO triggered a hybridization chain reaction, amplifying the fluorescence signal.[120] More recently, Xu *et al.* developed a PDA-nucleic acid nanoprobe for intracellular mRNA imaging and photothermal therapy. This system utilized catalytic hairpin assembly for signal amplification and precise cancer cell targeting.[121] The nanoprobe demonstrated high sensitivity, specificity, and the ability to distinguish between tumour and normal cells, while also leveraging PDA's photothermal properties for trigger cancer cell apoptosis under near-infrared irradiation.

9.5. Probing wettability of microplastics

Microplastics are initially hydrophobic when first dispersed in water. Our group discovered that the DNA adsorption properties of microplastics changed after soaking in water under mild conditions, such as room temperature for three months or at 85 °C for 30 minutes.[86] Raman spectroscopy of soaked microplastics showed no signs of oxidation compared to freshly dispersed microplastics, suggesting no chemical change. However, the soaked microplastics showed enhanced adsorption efficiency of SNA (Fig. 14a). It was found that microplastics had surface roughness features and nanosized pores capable of entrapping air. Soaking and heating caused the air bubbles to burst, enhancing the wettability of the microplastics. The more wettable surface allowed efficient contact between SNA and microplastics, resulting in higher binding capacity and affinity (Fig. 14b). Therefore, SNA can be used to investigate the wettability of microplastics.

10. Conclusions and future perspectives

In this article, we first reviewed fundamental interactions of DNA adsorption to various soft, polymeric and quantum materials, which notably lack metal ion components. As a result, most interactions are limited to relatively weak forces, including hydrogen bonds, π–π stacking, hydrophobic interactions, and van der Waals forces. These weak interactions allow the adsorbed DNA to remain functional for hybridization in most cases, unlike some inorganic nanomaterials that bind DNA too strongly and inhibit its chemical or biological functions.[32] With DNA attached, various applications become possible, ranging from biosensors to drug delivery systems. Based on the reviewed research, we have identified a few challenges and related future research opportunities.

1. Even though these materials lack metal ions, in many cases, metal ions present in buffer promote DNA adsorption. The involved metal ions are much lower than those typically present in inorganic materials, as metal ions only needed to be on the surface, thereby reducing potential toxicity. For example, mammalian cells naturally contain potassium (100–150 mM), sodium (10–20 mM), magnesium (~1 mM free, ~10–20 mM bound), and transition metal ions at much lower concentrations. The importance of metal coordination chemistry was further highlighted by the observation that transition metal ions promote DNA adsorption more effectively than alkaline earth metals. Advanced spectroscopic and computational techniques could provide deeper insights into how metal ions facilitate DNA binding, enabling the development of more selective and efficient hybrid materials systems.

2. Engineering the surface of materials can further promote DNA adsorption. For example, incorporating metal ions during the synthesis of PDA or functionalizing hydrogels with boronic acid was shown to enhance DNA adsorption. Further exploration of the synergistic effects of functional groups in DNA and surface modifications could lead to materials with improved adsorption capabilities, expanding their potential applications.

3. The pH-switchable and temperature–responsive properties of PDA and hydrogels offer exciting opportunities for designing smart DNA adsorption systems. Future research could focus on the development of stimuli-responsive materials that release DNA under specific conditions, such as changes in

pH, temperature, ionic strength and even specific molecules. Such systems could be particularly valuable for targeted drug delivery, where controlled release of DNA-based therapeutics precisely at disease sites is essential.

4. While the interactions between DNA and metal-free materials offer promising avenues for biosensing, several challenges must be addressed for practical applications. Achieving high selectivity and maintaining the conjugate stability remains critical, as competing interactions in complex biological environments (e.g., proteins, ions) can interfere with target recognition. Advances in stimuli-responsive systems (e.g., pH-switchable PDA) and polyvalent binding designs (e.g., SNAs) offer potential solutions. However, reproducibility and scalability for real-world sensing platforms demand continued exploration.

5. The successful selection of DNA aptamers for microplastics and cellulose highlights the potential to leverage intermediate DNA adsorption affinities of polymeric and quantum materials to achieve sequence-specific DNA binding. Further work on aptamer selections for other materials, such as hydrogels and PDA, is anticipated. This precise binding capability could be valuable for creating smart, functional materials with DNA-based coatings and for extraction of nucleic acids.

6. Finally, an interesting direction is the integration of hard and soft materials.[69] For instance, DNA can be utilized to control of the growth and polymerization of materials. A recent representative example is DNApatite, a novel DNA-templated apatite hybrid, that demonstrates how biomolecular templates can guide inorganic crystallization at the molecular level.[122] In DNApatite, DNA is not merely adsorbed, but integrated as a structural and functional component, maintaining molecular recognition ability while significantly improving mechanical robustness and stability. It would be interesting to examine whether DNA can be used to regulate the outcome of PDA and hydrogels via processes such as molecular imprinting. Such hybrid approaches could bridge the gap between soft, functional interfaces and durable, biocompatible frameworks, expanding the scope of DNA-based material applications into load-bearing biomedical devices and next-generation sensing platforms.

Author contributions

All of the authors contributed to the manuscript preparation. J. L. and J. L. conceived the outline of the manuscript. M. Z. wrote the original draft. J. L., and J. L. revise the manuscript.

Conflicts of interest

The authors declare no conflict of interest.

Data availability

No primary research results, software or code have been included and no new data were generated or analysed as part of this review.

Acknowledgements

References

1 W. Zhou, Y. Lim, H. Lin, S. Lee, Y. Li, Z. Huang, J. S. Du, B. Lee, S. Wang, A. Sánchez-Iglesias, M. Grzelczak, L. M. Liz-Marzán, S. C. Glotzer and C. A. Mirkin, *Nat. Mater.*, 2023, **23**, 424–428.

2 B. Liu and J. Liu, *Matter*, 2019, **1**, 825–847.

3 L. Li, H. Xing, J. Zhang and Y. Lu, *Acc. Chem. Res.*, 2019, **52**, 2415–2426.

4 A. A. Babadi, S. Rahmati, R. Fakhlaei, R. Heidari, S. Baradaran, M. Akbariqomi, S. Wang, G. Tavoosidana, W. Doherty and K. Ostrikov, *Sci. Rep.*, 2022, **12**, 1–12.

5 Z. Wu, W. Wen, F. Luo, F. Chen, Y. Xiong, X. Zhang and S. Wang, *Anal. Chem.*, 2021, **93**, 4506–4512.

6 C. Xue, S. Hu, Z. H. Gao, L. Wang, M. X. Luo, X. Yu, B. F. Li, Z. Shen and Z. S. Wu, *Nat. Commun.*, 2021, **12**, 1–12.

7 P. Yang, R. Zhou, C. Kong, L. Fan, C. Dong, J. Chen, X. Hou and F. Li, *ACS Nano*, 2021, **15**, 16870–16877.

8 W. Zhou, R. Saran and J. Liu, *Chem. Rev.*, 2017, **117**, 8272–8325.

9 H. Yu, O. Alkhamis, J. Canoura, Y. Liu and Y. Xiao, *Angew. Chem., Int. Ed.*, 2021, **60**, 16800–16823.

10 H. M. Meng, T. Fu, X. B. Zhang and W. Tan, *Natl. Sci. Rev.*, 2015, **2**, 71–84.

11 K. Yang, N. M. Mitchell, S. Banerjee, Z. Cheng, S. Taylor, A. M. Kostic, I. Wong, S. Sajjath, Y. Zhang, J. Stevens, S. Mohan, D. W. Landry, T. S. Worgall, A. M. Andrews and M. N. Stojanovic, *Science*, 2023, **380**, 942–948.

12 S. Stangherlin, N. Lui, J. H. Lee and J. Liu, *TrAC Trends Anal. Chem.*, 2025, **191**, 118349.

13 Y. Li and R. R. Breaker, *J. Am. Chem. Soc.*, 1999, **121**, 5364–5372.

14 J. Liu, *Phys. Chem. Chem. Phys.*, 2012, **14**, 10485–10496.

15 B. Liu, L. Ma, Z. Huang, H. Hu, P. Wu and J. Liu, *Mater. Horiz.*, 2018, **5**, 65–69.

16 C. Lu, Y. Liu, Y. Ying and J. Liu, *Langmuir*, 2017, **33**, 630–637.

17 W. Ji, D. Li, W. Lai, X. Yao, M. F. Alam, W. Zhang, H. Pei, L. Li and A. R. Chandrasekaran, *Langmuir*, 2019, **35**, 5050–5053.

18 C. W. Smith, M. S. Hizir, N. Nandu and M. V. Yigit, *Anal. Chem.*, 2022, **94**, 1195–1202.

19 C. W. Smith, M. J. Kachwala, R. L. Cole and M. V. Yigit, *ACS Food Sci. Technol.*, 2022, **2**, 1217–1223.

20 J. K. Patra, G. Das, L. F. Fraceto, E. V. R. Campos, M. D. P. Rodriguez-Torres, L. S. Acosta-Torres, L. A. Diaz-Torres, R. Grillo, M. K. Swamy, S. Sharma, S. Habtemariam and H. S. Shin, *J. Nanobiotechnol.*, 2018, **16**, 1–33.

21 D. Hauser, D. Septiadi, J. Turner, A. Petri-Fink and B. Rothen-Rutishauser, *Mater.*, 2020, **13**, 1730.

22 S. Cai, Y. Cheng, C. Qiu, G. Liu and C. Chu, *Smart Mater. Med.*, 2023, **4**, 294–312.

23 S. Correa, A. K. Grosskopf, H. Lopez Hernandez, D. Chan, A. C. Yu, L. M. Stapleton and E. A. Appel, *Chem. Rev.*, 2021, **121**, 11385–11457.

24 F. Poustchi, H. Amani, Z. Ahmadian, S. V. Niknezhad, S. Mehrabi, H. A. Santos and M. A. Shahbazi, *Adv. Healthc. Mater.*, 2021, **10**, 2001571.

25 T. S. M. Amelia, W. M. Khalik, M. C. Ong, Y. T. Shao, H. J. Pan and K. Bhubalan, *Prog. Earth Planet. Sci.*, 2021, **8**, 1–26.

26 E. Winiarska, M. Jutel and M. Zemelka-Wiacek, *Environ. Res.*, 2024, **251**, 118535.

27 E. Jeong, J. Y. Lee and M. Redwan, *Emerg. Contam.*, 2024, **10**, 100369.

28 Y. Wu and T. Weil, *Adv. Sci.*, 2022, **9**, 2200059.

29 M. P. Kushalkar, B. Liu and J. Liu, *Langmuir*, 2020, **36**, 11183–11195.

30 Y. Zhou, Z. Huang, R. Yang and J. Liu, *Chem.–Eur. J.*, 2018, **24**, 2525–2532.

31 T. M. Herne and M. J. Tarlov, *J. Am. Chem. Soc.*, 1997, **119**, 8916–8920.

32 F. Zhang, S. Wang and J. Liu, *Anal. Chem.*, 2019, **91**, 14743–14750.

33 K. M. Koo, A. A. I. Sina, L. G. Carrascosa, M. J. A. Shiddiky and M. Trau, *Anal. Methods*, 2015, **7**, 7042–7054.

34 J. M. Carnerero, A. Jimenez-Ruiz, P. M. Castillo and R. Prado-Gotor, *ChemPhysChem*, 2017, **18**, 17–33.

35 B. Liu and J. Liu, *Anal. Methods*, 2017, **9**, 2633–2643.

36 B. Liu and J. Liu, *TrAC Trends Anal. Chem.*, 2019, **121**, 115690.

37 S. Sawan, A. Errachid, R. Maalouf and N. Jaffrezic-Renault, *TrAC Trends Anal. Chem.*, 2022, **157**, 116748.

38 Q. ul A. Zahra, S. Ullah, F. Shahzad, B. Qiu, X. Fang, A. Ammar, Z. Luo and S. Abbas Zaidi, *Prog. Mater. Sci.*, 2022, **129**, 100967.

39 B. Liu, S. Salgado, V. Maheshwari and J. Liu, *Curr. Opin. Colloid Interface Sci.*, 2016, **26**, 41–49.

40 A. Lopez and J. Liu, *Adv. Intell. Syst.*, 2020, **2**, 2000123.

41 E. Roth, A. Glick Azaria, O. Girshevitz, A. Bitler and Y. Garini, *Nano Lett.*, 2018, **18**, 6703–6709.

42 N. Varghese, U. Mogera, A. Govindaraj, A. Das, P. K. Maiti, A. K. Sood and C. N. R. Rao, *ChemPhysChem*, 2009, **10**, 206–210.

43 P. Shih, L. G. Pedersen, P. R. Gibbs and R. Wolfenden, *J. Mol. Biol.*, 1998, **280**, 421–430.

44 R. Nutiu and Y. Li, *J. Am. Chem. Soc.*, 2003, **125**, 4771–4778.

45 M. Zandieh, X. Luo, Y. Zhao, C. Feng and J. Liu, *Angew. Chem., Int. Ed.*, 2024, e202421438.

46 H. Lee, S. M. Dellatore, W. M. Miller and P. B. Messersmith, *Science*, 2007, **318**, 426–430.

47 J. Bolaños-Cardet, D. Ruiz-Molina, V. J. Yuste and S. Suárez-García, *Chem. Eng. J.*, 2024, **481**, 148674.

48 V. Ball, *Front. Bioeng. Biotechnol.*, 2018, **6**, 398821.

49 Y. Wang, X. Ma, C. Ding and L. Jia, *Anal. Chim. Acta*, 2015, **862**, 33–40.

50 Z. Zhong, X. Yao, X. Gao and L. Jia, *Anal. Biochem.*, 2017, **534**, 14–18.

51 Z. Wang, Y. Xie, Y. Li, Y. Huang, L. R. Parent, T. Ditri, N. Zang, J. D. Rinehart and N. C. Gianneschi, *Chem. Mater.*, 2017, **29**, 8195–8201.

52 M. P. Kushalkar, B. Liu and J. Liu, *Langmuir*, 2020, **36**, 11183–11195.

53 M. Zandieh and J. Liu, *Langmuir*, 2020, **36**, 3260–3267.

54 M. Zandieh and J. Liu, *Langmuir*, 2021, **37**, 8953–8960.

55 M. Zandieh, B. M. Hagar and J. Liu, *Part. Part. Syst. Charact.*, 2021, **37**, 2000208.

56 M. Zandieh and J. Liu, *Langmuir*, 2020, **36**, 14324–14332.

57 M. Mammen, S.-K. Choi, G. M. Whitesides and K. Choi, *Angew. Chem., Int. Ed.*, 1998, **37**, 2754–2794.

58 M. Labieniec and T. Gabryelak, *J. Photochem. Photobiol. B*, 2006, **82**, 72–78.

59 C. Wang, J. Zhou, P. Wang, W. He and H. Duan, *Bioconjug. Chem.*, 2016, **27**, 815–823.

60 M. M. Azab, R. Cherif, A. L. Finnie, M. M. Abou El-Alamin, M. A. Sultan and A. W. Wark, *Analyst*, 2018, **143**, 1635–1643.

61 J. I. Cutler, E. Auyeung and C. A. Mirkin, *J. Am. Chem. Soc.*, 2012, **134**, 1376–1391.

62 J. Yang, V. Saggiomo, A. H. Velders, M. A. C. Stuart and M. Kamperman, *PLoS One*, 2016, **11**, e0166490.

63 J. Sedõ, J. Saiz-Poseu, F. Busqué and D. Ruiz-Molina, *Adv. Mater.*, 2013, **25**, 653–701.

64 Y. Zhu, S. Li, J. Li, N. Falcone, Q. Cui, S. Shah, M. C. Hartel, N. Yu, P. Young, N. R. de Barros, Z. Wu, R. Haghniaz, M. Ermis, C. Wang, H. Kang, J. Lee, S. Karamikamkar, S. Ahadian, V. Jucaud, M. R. Dokmeci, H. J. Kim and A. Khademhosseini, *Adv. Mater.*, 2022, **34**, 2108389.

65 Y. Liang, J. He and B. Guo, *ACS Nano*, 2021, **15**, 12687–12722.

66 D. Liu, C. Huyan, Z. Wang, Z. Guo, X. Zhang, H. Torun, D. Mulvihill, B. Bin Xu and F. Chen, *Mater. Horiz.*, 2023, **10**, 2800–2823.

67 X. Yao, S. Zhang, L. Qian, N. Wei, V. Nica, S. Coseri and F. Han, *Adv. Funct. Mater.*, 2022, **32**, 2204565.

68 H. Song, D. H. Jung, S. Y. Jeong, S. H. Kim, H. H. Cho, R. Khadka, J. H. Heo and J. H. Lee, *Adv. Compos. Hybrid Mater.*, 2024, **7**, 1–13.

69 H. Song, D. H. Jung, Y. Cho, H. H. Cho, V. G. Panferov, J. Liu, J. H. Heo and J. H. Lee, *Coord. Chem. Rev.*, 2025, **541**, 216835.

70 R. Narayanaswamy and V. P. Torchilin, *The Road from Nanomedicine to Precision Medicine*, 2020, pp. 1117–1150.

71 C. D. Spicer, *Polym. Chem.*, 2020, **11**, 184–219.

72 P. A. Mistry, M. N. Konar, S. Latha, U. Chadha, P. Bhardwaj and T. K. Eticha, *Int. J. Polym. Sci.*, 2023, 4717905.

73 S. Mitura, A. Sionkowska and A. Jaiswal, *J. Mater. Sci. Mater. Medicine*, 2020, **31**, 1–14.

74 A. López-Díaz, A. S. Vázquez and E. Vázquez, *ACS Nano*, 2024, **18**, 20817–20826.

75 J. Liu, *Soft Matter*, 2011, **7**, 6757–6767.

76 L. Zhao, L. Li, G. Yang, B. Wei, Y. Ma and F. Qu, *Biosens. Bioelectron.*, 2021, **194**, 113597.

77 Y. Zhang, L. Zhu, J. Tian, L. Zhu, X. Ma, X. He, K. Huang, F. Ren and W. Xu, *Adv. Sci.*, 2021, **8**, 2100216.

78 M. Emin Çorman, N. Bereli, S. Özkara, L. Uzun and A. Denizli, *Biomed. Chromatogr.*, 2013, **27**, 1524–1531.

79 C. Lu, Z. Huang, B. Liu, Y. Liu, Y. Ying and J. Liu, *Angew. Chem., Int. Ed.*, 2017, **56**, 6208–6212.

80 A. Lopez, Y. Zhao, Z. Huang, Y. Guo, S. Guan, Y. Jia and J. Liu, *Adv. Mater. Interfaces*, 2020, **8**, 2001798.

81 K. Erol, *J. Macromol. Sci.*, 2016, **53**, 629–635.

82 Y. Li, Z. Zhang, B. Liu and J. Liu, *Langmuir*, 2019, **35**, 13727–13734.

83 Y. Huang, S. Li, L. W. C. Zettle, Y. Ma, H. E. Naguib and E. Kumacheva, *Nanoscale*, 2023, **15**, 14531–14542.

84 M. Zandieh, K. Patel and J. Liu, *Langmuir*, 2022, **38**, 1915–1922.

85 L. Wu, K. Patel, M. Zandieh and J. Liu, *Microplastics*, 2023, **2**, 158–167.

86 M. Zandieh, Ú. E. Hogan, R. D. L. Smith and J. Liu, *Langmuir*, 2023, **39**, 4959–4966.

87 G. P. Gopalan, A. Suku and S. Anas, *Handbook of Biomass*, 2024, pp. 877–917.

88 S. Zhang, J. Xu, J. Xu, Y. Ming, L. Ding, L. Wu, X. Liu, Z. Du and S. Jiang, *ACS Appl. Nano Mater.*, 2024, **7**, 20229–20239.

89 Q. Fang, H. N. Sun, M. Zhang, T. H. Mu and M. Garcia-Vaquero, *ACS Agric. Sci. Technol.*, 2025, **5**, 3–27.

90 S. Zhang, J. Xu, J. Xu, Y. Ming, L. Ding, L. Wu, X. Liu, Z. Du and S. Jiang, *ACS Appl. Nano Mater.*, 2024, **7**, 20229–20239.

91 M. Mariano, N. Naseri, D. M. Do Nascimento, L. Franqui, A. B. Seabra, A. P. Mathew and J. S. Bernardes, *ACS Appl. Bio. Mater.*, 2024, **7**, 8377–8388.

92 S. Su, R. Nutiu, C. D. M. Filipe, Y. Li and R. Pelton, *Langmuir*, 2007, **23**, 1300–1302.

93 T. Sato, M. M. Ali, R. Pelton and E. D. Cranston, *Biomacromol.*, 2012, **13**, 3173–3180.

94 M. Mujtaba, M. Kaya, L. Akyuz, D. Erdonmez, B. Akyuz and I. Sargin, *Int. J. Biol. Macromol.*, 2017, **102**, 914–923.

95 T. Zhong, G. Jian, Z. Chen, M. Wolcott, S. Nassiri and C. A. Fernandez, *Nanotechnol. Rev.*, 2022, **11**, 2673–2713.

96 B. J. Boese and R. R. Breaker, *Nucleic Acids Res.*, 2007, **35**, 6378–6388.

97 B. J. Boese, K. Corbino and R. R. Breaker, *Nucleosides Nucleotides Nucleic Acids*, 2008, **27**, 949–966.

98 X.-Q. Zhang, M. Chen, R. Lam, X. Xu, E. Osawa and D. Ho, *ACS Nano*, 2009, **3**, 2609–2616.

99 K. A. Laptinskiy, E. N. Vervald, A. N. Bokarev, S. A. Burikov, M. D. Torelli, O. A. Shenderova, I. L. Plastun and T. A. Dolenko, *J. Phys. Chem. C*, 2018, **122**, 11066–11075.

100 M. Zandieh and J. Liu, *Langmuir*, 2023, **39**, 11596–11602.

101 V. Chakrapani, J. C. Angus, A. B. Anderson, S. D. Wolter, B. R. Stoner and G. U. Sumanasekera, *Science*, 2007, **318**, 1424–1430.

102 D. A. Hines and P. V. Kamat, *ACS Appl. Mater. Interfaces*, 2014, **6**, 3041–3057.

103 H. Shabbir, E. Csapó and M. Wojnicki, *Inorganics*, 2023, **11**, 262.

104 Y. Wang and A. Hu, *J. Mater. Chem. C Mater.*, 2014, **2**, 6921–6939.

105 N. Ullal, R. Mehta and D. Sunil, *Analyst*, 2024, **149**, 1680–1700.

106 F. Li, Q. Cai, X. Hao, C. Zhao, Z. Huang, Y. Zheng, X. Lin and S. Weng, *RSC Adv.*, 2019, **9**, 12462–12469.

107 G. Han, J. Zhao, R. Zhang, X. Tian, Z. Liu, A. Wang, R. Liu, B. Liu, M. Y. Han, X. Gao and Z. Zhang, *Angew. Chem., Int. Ed.*, 2019, **58**, 7087–7091.

108 C. H. Lu, H. H. Yang, C. L. Zhu, X. Chen and G. N. Chen, *Angew. Chem., Int. Ed.*, 2009, **48**, 4785–4787.

109 A. H. Loo, Z. Sofer, D. Bouša, P. Ulbrich, A. Bonanni and M. Pumera, *ACS Appl. Mater. Interfaces*, 2016, **8**, 1951–1957.

110 Q. Wei, P. Zhang, T. Liu, H. Pu and D. W. Sun, *Food Chem.*, 2021, **356**, 129668.

111 J. Wang, X. Li, H. Lei and J. Liu, *Anal. Chem.*, 2025, **97**, 9454–9461.

112 Z. Fei, N. Gupta, M. Li, P. Xiao and X. Hu, *Sci. Adv.*, 2023, **9**, 19.

113 L. Zhang, R. N. Deraney and A. Tripathi, *Biomicrofluidics*, 2015, **9**, 064118.

114 M. Zandieh and J. Liu, *Bioconjug. Chem.*, 2021, **32**, 801–809.

115 D. Baek, S. Y. Joe, H. Shin, C. Park, S. Jo and H. Chun, *Biochip J.*, 2024, **18**, 357–372.

116 T. Ding, Y. Xiao, Q. Saiding, X. Li, G. Chen, T. Zhang, J. Ma and W. Cui, *Adv. Mater.*, 2024, **36**, 2403557.

117 V. Petrakova, V. Benson, M. Buncek, A. Fiserova, M. Ledvina, J. Stursa, P. Cigler and M. Nesladek, *Nanoscle*, 2016, **8**, 12002.

118 W. Qiang, H. Hu, L. Sun, H. Li and D. Xu, *Anal. Chem.*, 2015, **87**, 12190–12196.

119 C. K. K. Choi, J. Li, K. Wei, Y. J. Xu, L. W. C. Ho, M. Zhu, K. K. W. To, C. H. J. Choi and L. Bian, *J. Am. Chem. Soc.*, 2015, **137**, 7337–7346.

120 D. He, X. He, X. Yang and H. W. Li, *Chem. Sci.*, 2017, **8**, 2832–2840.

121 J. Xu, X. Zhong, M. Fan, Y. Xu, Y. Xu, S. Wang, Z. Luo and Y. Huang, *Anal. Bioanal. Chem.*, 2024, **416**, 849–859.

122 J. W. Lee, B. Lee, C. H. Park, J. H. Heo, T. Y. Lee, D. Lee, J. Bae, P. R. Sundharbaabu, W. K. Yeom, S. Chae, J.-H. Lim, S.-W. Lee, J.-S. Choi, H.-B. Bae, J.-Y. Choi, E.-H. Lee, D. S. Yoon, G. Y. Yeom, H. Shin and J. H. Lee, *Adv. Mater.*, 2024, **36**, 2470329.